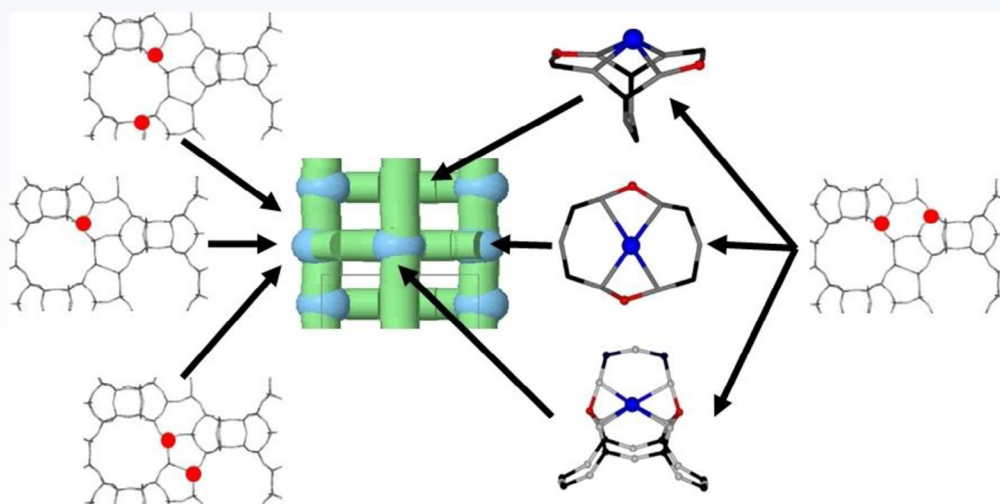


50 Tuning the Aluminum Distribution in Zeolites to Increase their Performance in Acid-Catalyzed Reactions



Jiri Dědeček, Edyta Tabor,* and Stepan Sklenak^[a]



The organization of Al atoms in the framework of Si-rich zeolites is very important and includes two classes: (i) the Al siting that determines which individual, crystallographically distinguishable framework T sites are occupied by Al atoms and (ii) the Al distribution, which describes the relation of two or more Al atoms in the framework, their distances, and the possibility of neighboring Al atoms to cooperate in the formation

of active sites. The organization of Al significantly affects the catalytic properties of Si-rich, zeolite-based catalysts in acid and redox catalysis. Herein, what is known about the organization of Al in the framework of industrially very important pentasil-ring Si-rich zeolites (ZSM-5, beta zeolite, mordenite, ferrierite, MCM-22, and TNU-9), as well as the very promising SSZ-13 Si-rich zeolite with the CHA structure, is summarized.

1. Introduction

Zeolites today represent the broadest and most important group of heterogeneous industrial catalysts.^[1] They are used in a wide range of acid-catalyzed reactions for the transformation of hydrocarbons and their derivatives that are relevant for the petrochemical industry, as well as in the synthesis of fine chemicals.^[2] Cationic zeolite forms are used as redox catalysts for NO_x elimination from diesel exhausts and process gases and for N₂O abatement.^[3] Moreover, zeolites in the protonic and cationic forms were recently reported to be promising catalysts in the utilization of biomass and renewables,^[4] in the conversion of methane into valuable products, and in the utilization of carbon dioxide.^[5]

The enormously wide application of zeolites in catalysis results from a unique combination of the properties of zeolites. Their microporous crystalline aluminosilicate frameworks are composed of corner-sharing TO₄ tetrahedra (T = Si, Al).^[6] Variability in the arrangements of the TO₄ tetrahedra results in more than 200 known zeolite topologies with different microporous channel and cavity systems.^[7] Thus, zeolites assume the role of chemically, thermally, and mechanically stable matrices that are also rigid and well-defined at the atomic scale. Moreover, zeolites represent a highly variable microporous system with tunable properties. Framework Al/Si substitutions introduce a negative charge to the silicate framework. This negative charge has to be compensated by extra-framework cationic species—protons, metal, and metal-oxo cations. These exchangeable, positively charged extra-framework species can act as catalytic and sorption centers. The extremely wide range and also variable nature of extra-framework cationic species (i.e., Brønsted and Lewis acids, various redox and base centers)^[6b,8] acting as active sites in tandem with the tunable geometry and the architecture of the pore structure result in an enormously broad array of possible zeolite applications in catalytic processes. The structure of the pore system is responsible

for the shape selectivity controlled by the transition states and the transport of the reactants and products through the pores. As mentioned above, the active sites balance the negative charge of the AlO₄⁻ species in the zeolite framework. Therefore, the organization of Al atoms in the zeolite framework determines the location, distances, properties, and nature of the active sites in the zeolite catalysts. The organization of Al includes two features that are relevant for Si-rich matrices. First, the Al siting in individual crystallographically distinguishable framework T sites controls the location of monovalent active sites in the zeolite channel/cavity system and also governs the local arrangement of the active sites regarding the nearest pore structure.^[9] This in turn controls the intimate confinement of the reactants and transition states in the pore void volume.^[8a] Second, the Al distribution describes the relation of two or more Al atoms in the framework, their distances, and the possibility of neighboring Al atoms to cooperate in the formation of active sites.^[8a,10] Thus, the Al distribution significantly affects the formation and the location of polyvalent active sites and the cooperation of the monovalent sites, including protons. Furthermore, it influences the local arrangement of the polyvalent active site or two cooperating monovalent sites, the possibility of their cooperation, their nearest pore geometry, and thus the intimate confinement of the reactants and transition states in the pore void. Figure 1 shows various types of active sites related to one and two Al atoms.

Recent research clearly shows that the organization of Al (both Al siting and Al distribution) in the zeolite framework is not random or controlled by some simple rules but is instead

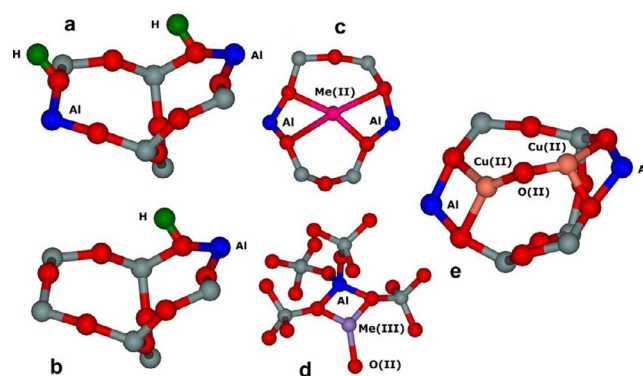


Figure 1. Schematic depiction of some types of active sites related to one and two Al atoms. a) Two close protonic sites, b) isolated protonic site, c) bare M²⁺ cations in different rings, d) monovalent [M³⁺-O²⁻]⁺ oxo-species, and e) Cu²⁺-O-Cu²⁺ bridging structure.

[a] Dr. J. Dědeček, Dr. E. Tabor, Dr. S. Sklenak
J. Heyrovský Institute of Physical Chemistry, Czech Academy of Sciences
Dolejškova 2155/3, 182 23 Prague 8 (Czech Republic)
E-mail: edyta.tabor@jh-inst.cas.cz

The ORCID identification number(s) for the author(s) of this article can be found under:
<https://doi.org/10.1002/cssc.201801959>.

This publication is part of a Special Issue focusing on "Celebrating 50 years of the Jerzy Haber Institute of Catalysis and Surface Chemistry of the Polish Academy of Sciences". Please visit the issue at <http://doi.org/10.1002/cssc.v12.3>.

governed by the conditions used during the synthesis of the zeolites.^[8a,11] This findings has opened various possibilities to optimize zeolite-based catalysts by tuning the organization of Al in the zeolite and to develop new generations of highly active and selective catalysts/catalytic processes.^[8a,10b,12] Significant achievements have been achieved in the analysis and control of the distribution of Al in zeolites in recent years. Thus, this Review is devoted to this subject to facilitate applications of this knowledge in the field of catalysis.

Jiri Dědeček received his Ph.D. degree at the J. Heyrovský Institute of Physical Chemistry, Prague, and his D.Sc. degree at the Academy of Sciences of the Czech Republic. After a postdoctoral fellowship at Lehigh University, Bethlehem, PA, USA, he became a scientist at the J. Heyrovský Institute of Physical Chemistry, where he is currently leading the Department of Structure and Dynamics in Catalysis. His current research focuses on acid–base and redox heterogeneous catalysis, the synthesis of aluminosilicate molecular sieves, and the application of spectroscopic methods (MAS NMR, UV/Vis absorption/emission, and FTIR) in the characterization of catalysts at the atomic level.



Edyta Tabor received her Ph.D. degree at the Jerzy Haber Institute of Catalysis and Surface Chemistry in Kraków in the field of homogeneous oxidation catalysis under the guidance of Prof. Jerzy Haber. She held her postdoctoral fellowship at the J. Heyrovský Institute of Physical Chemistry in Prague. Her research focuses on the spectroscopic elucidation of zeolite-based catalysts and their performance in acid–base and redox reactions.



Stepan Sklenak has been a Senior Scientist at the J. Heyrovsky Institute of Physical Chemistry, Prague, Czech Republic since 2004. After obtaining his Ph.D. degree in 1995, he spent almost a decade at the Technion—Israel Institute of Technology, Yale University, the University of California, and Michigan State University. His current research focuses on the quantum-chemical calculations of zeolites to model their structure, reactivity, catalytic activity, and properties.



2. Classification of the Al Distribution in Si-Rich Zeolites

Only one type of the Al organization can be conclusively excluded from the zeolite family—two Al atoms connected by an oxygen bridge in an Al–O–Al structure. Such species have never been observed in zeolites or in any other aluminosilicate material (Loewenstein rule).^[6b,13] In the case of Al-rich materials (zeolites A, X, and Y; chabazite; etc.), the high Al content in the framework causes most Al atoms to be separated by only one Si atom.^[4b,14] Conversely, a low Al content in Si-rich zeolites allows a huge variety of Al arrangements, and according to the present knowledge, there are no restrictions in this area.^[8a]

Classification of the Al distribution results from a combination of the catalytic point of view (historically mainly related to the use of metallozeolites in redox catalysis) and the available analytical methods, as follows: 1) arrangement of Al atoms in aluminosilicate chains; 2) possibility to accommodate various types of divalent cationic species; 3) possibility of cooperation between two Al-related acid sites. These parameters are not unambiguously connected with the distance of the Al atoms.

Regarding point 1, we can identify only two Al atoms separated by only one Si atom. Thus, we can distinguish AlSiAl sequences from AlSi_n>1Al sequences. The Al atoms of AlSiAl sequences can be arranged in one or two rings and in one or more channels/cavities. The two Al atoms have various possibilities for cooperation and can exhibit various Al–Al distances. Note that the distance of the Al atoms in an AlSi₃Al sequence arranged linearly along the channel can be longer than the distance of the Al atoms in an AlSi₅Al sequence arranged on the perimeter of the zeolite channel. Figure 2 schematically depicts the types of Al distances in zeolites.

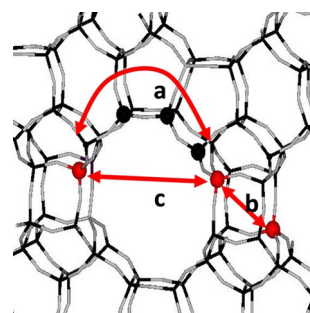


Figure 2. Schematic depiction of the types of Al distances in zeolites. a) Distance by the SiAl sequence, b) geometrical distance, and c) visible distance.

Concerning point 2, the main criterion for the description of the Al arrangement in the zeolite represents a possibility of two Al atoms to accommodate divalent cationic species—smaller bare divalent (Co^{2+}) cations in the dehydrated zeolite or hexaaqua complexes of such cations $[\text{Co}^{2+}(\text{H}_2\text{O})_6]$.^[8a,10a,15] This combines the distance of the Al atoms in an AlSi_nAl chain with their location in one or two rings and one or two channels.

In terms of point 3, the possibility of the cooperation of two Al-related acid sites does not reflect the length of the AlSi_nAl

chain or the location of Al in the rings, but only the distance of the Al atoms through the empty space of the zeolite channel.

Note that the above classification was first developed for ZSM-5 zeolite and was then continuously extended to other pentasil-ring zeolites.^[8a] Recently, the synthesis of Si-rich zeolites of a family other than the pentasil-ring family (ABC-6 family) was reported, and the Al distribution in these materials was analyzed.^[16] The study required actualization of the definition of the individual types of Al species, as shown below.

2.1. AlSiAl sequences

These Al species are well known for Al-rich matrices such as faujasite and A-type zeolites, but they are only rarely reported for Si-rich materials ($\text{Si}/\text{Al} > 5$), and their relation to the zeolite properties is typically discussed separately for individual cases.^[17] There are two possible ways in which AlSiAl sequences can be arranged in the zeolite framework:

- 1) Both Al atoms face the same channel. In this case, the Al atoms are able to accommodate both Co^{2+} hexaaqua complexes and bare Co^{2+} cations, and the acid sites related to them can cooperate in acid-catalyzed reactions.^[17c]
- 2) Each Al atom of the AlSiAl sequence faces different channels. Such an arrangement is possible only in zeolites with a wall formed by bilayers of TO_4 tetrahedra (typically pentasil-ring zeolites). In this case, the Al atoms cannot accommodate Co^{2+} hexaaqua complexes or bare Co^{2+} cations, and the acid sites related to the Al atoms cannot cooperate. From the point of view of both acid and redox catalysis, these Al atoms exhibit behavior of distant isolated Al atoms.^[17d] Figure 3 depicts AlSiAl sequences in which the two Al atoms face either the same channel or different channels.

2.1.1. Al triads (Al_{TR})

AlSiAlSiAl sequences represent a specific case of AlSiAl atoms located in the silica environment in zeolites with walls formed by a single layer of TO_4 tetrahedra. Owing to the odd number of Al atoms in this sequence, the isolated Al triad is able to accommodate only one divalent cation. Conversely, the acid sites related to all three Al atoms have to be close enough to cooperate in acid-catalyzed reactions.^[16]

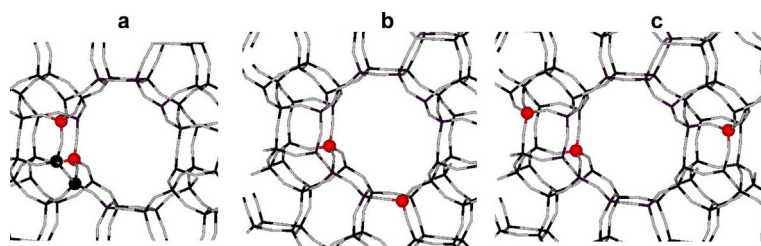


Figure 4. Schematic representations of a) Al pairs, b) close unpaired Al atoms, and c) single Al atoms.

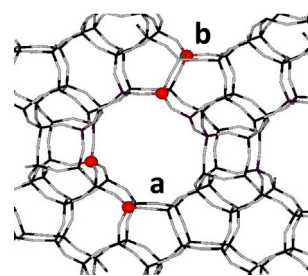


Figure 3. AlSiAl sequences with the two Al atoms facing a) the same or b) different channels.

2.2. Other types of Al distribution

In contrast to AlSiAl sequences, the following types of Al distribution are defined in terms of their behavior with regard to the accommodation of divalent cations.

2.2.1. Al pairs (Al_{PAIR})

Al pairs represent two Al atoms located in one zeolite ring that are able to accommodate both Co^{2+} hexaaqua complexes and bare Co^{2+} cations.^[8a,10a,18] The acid sites related to these Al atoms can cooperate in acid-catalyzed reactions. The Al atoms of these Al pairs should be separated by two or three Si atoms (AlSi_2Al or AlSi_3Al sequences). Whereas the presence of AlSi_2Al sequences has been confirmed for a number of zeolites, the formation of AlSi_3Al sequences is rare. Recently, they have been proven for SSZ-13, but they represent only a minor Al species in that zeolite.^[16] We can also speculate on their formation in zeolites in other frameworks with Al pairs (sites for divalent cations) located in the 8-ring, for example, mordenite. Note that there is not a simple way by which they can be distinguished from AlSi_2Al sequences in the same ring. Figure 4 shows the schematic representations of Al pairs, close unpaired Al atoms, and single Al atoms.

2.2.2. Close unpaired Al atoms (Al_{CLOSE})

Close unpaired Al atoms are able to accommodate Co^{2+} hexaaqua complexes, but they are unable to form cationic sites for bare Co^{2+} cations.^[8a,16,19] We can speculate that acid sites related to these Al atoms can cooperate in acid-catalyzed reactions. The two Al atoms of $\text{AlSi}_{n>1}\text{Al}$ sequences are suggested to be located in two rings close enough to accommodate a Co^{2+} hexaaqua complex. The stabilization energy of bare M^{2+}

containing only one Al atom (with the second one located in a different ring) is very low,^[20] and the highly reactive M^{2+} cation most likely forms monovalent (oxo)species (e.g. $[M^{2+}OH^-]^+$ or $[M^{3+}O^{2-}]^+$, see Refs. [17d,19,21]). A second possibility of the arrangement of this species in the zeolite framework corresponds to the two Al atoms of $AlSi_3Al$ sequences located in an 8-ring with the ring geometry not providing a site for a bare divalent cation but only for the highly reactive M^{2+} cation that forms some oxo species.

2.2.3. Single Al atoms (Al_{SINGLE})

The Al atoms of $AlSi_{n>3}Al$ sequences are located so far from each other that they do not accommodate either bare Co^{2+} cations or Co^{2+} hexaaqua complexes, and the Al atoms of these sequences can be regarded as isolated.^[8a,10a,18] The acid sites related to these Al atoms are suggested to be unable to cooperate in acid-catalyzed reactions of smaller molecules. Note that this aspect is not (in contrast to that previously discussed) exactly defined and can vary for different lengths of involved molecules. $AlSi_{n>7}Al$ sequences with Al atoms located in two different zeolite channels represent another possibility for the arrangement of single Al atoms.

2.2.4. Two Al atoms in the hexagonal prism

The two Al atoms of some $AlSi_{n>1}Al$ sequence can be located in different rings of the hexagonal prism or in a similar structure (the beta cage of beta zeolite).^[7] These Al atoms are able to accommodate bare Co^{2+} cations but not Co^{2+} hexaaqua complexes.^[22] The acid sites connected with these Al atoms are believed not to cooperate in acid-catalyzed reactions. Each of these Al atoms can also accommodate monovalent cationic species in the ring in which the Al atom is located. Bare divalent cations accommodated in these sites are not accessible to guest molecules owing to the fact that access to the cation is possible only through the 6-ring or even a smaller ring. Thus, upon analyzing the Al distribution in zeolites, these Al atoms have to be regarded as isolated. Figure 5 shows two Al atoms in D6R (i.e., double 6-ring).

2.2.5. Other possibilities

Note that other possibilities of the Al distribution in Si-rich zeolites can be suggested if more than two Al atoms are considered. Analogously to $AlSiAl$ triads, the arrangement of three close atoms forming one Al pair or two close unpaired Al

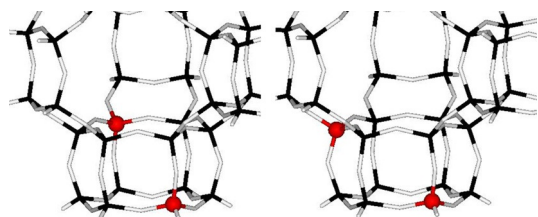


Figure 5. Two Al atoms in D6R.

atoms with a close third Al atom can also be considered. However, methods for evidence of such species have not yet been developed, and we can only speculate on the presence of such Al species in zeolites. Nevertheless, the low content of framework Al in Si-rich zeolites makes the occurrence of such Al species improbable. Note that the abovementioned Al triads have been reported for a highly specific method for the synthesis of SSZ-13, moreover, with a relatively high content of framework Al. Conversely, the arrangement of four Al atoms into two Al pairs enabling the cooperation of two bare divalent cations has unambiguously been proven in ferrierite.^[23]

3. Methods to Analyze the Al Distribution in Si-Rich Zeolites

The methods described in this chapter result from the need to analyze the organization of Al in some zeolites (ZSM-5, ferrierite, mordenite, beta zeolite, TNU-9, and SSZ-13) that have appeared during the last decades.^[8a,16,24] The developed methods are, therefore, without doubt affected by the nature of the investigated matrices. Thus, analysis of the distribution of Al in new matrices requires, at a minimum, modification of the approaches described and will eventually require the development of new methods.

3.1. ^{29}Si MAS NMR spectroscopy for analysis of $AlSiAl$ sequences

^{29}Si magic angle spinning (MAS) NMR spectroscopy represents the oldest method used to analyze the Al distribution in zeolites. It is connected with the analysis of the organization of Al in Al-rich zeolites (e.g., A-type and zeolites X and Y).^[14,25] ^{29}Si MAS NMR spectroscopy allows the individual types of $Si(nSi,4-nAl)$ atoms ($n=0-4$) to be discriminated (for details, see Refs. [6b,26]). However, the presence of Si atoms with $n < 3$ in the framework does not unambiguously reflect the arrangement of the $AlSiAl$ atoms. The $AlSiAl$ sequence can be arranged in Si-rich matrices in different ways, and only a rough estimate of the limit values of the $AlSiAl$ concentration can be made. Figure 6 shows the ^{29}Si MAS NMR spectrum of a zeolite with $Si(nSi,4-nAl)$ atoms ($n=1-4$). Figure 7 reveals a schematic depiction of an isolated $AlSiAl$ sequence, an $AlSiAl$ sequence in a ring or an infinite chain, and an $AlSiAl$ sequence in an isolated triad.

The first possibility of the arrangement of $(AlSi)_n$ sequences in Si-rich zeolites represents isolated $AlSiAl$ sequences in the all-silica environment. One $Si(2Si,2Al)$ and six $Si(1Si,3Al)$ atoms correspond to two Al atoms of the $AlSiAl$ sequence in this case. This arrangement corresponds to the upper bound of the concentration of Al atoms in the $AlSiAl$ sequences in the zeolite. The concentration of Al atoms in these isolated sequences (in % of all Al atoms) is given by Equation (1):

$$Al_{AlSiAl} [\%] = \frac{2I_2}{(1.25I_2 + 0.25I_1)} \times 100\% \quad (1)$$

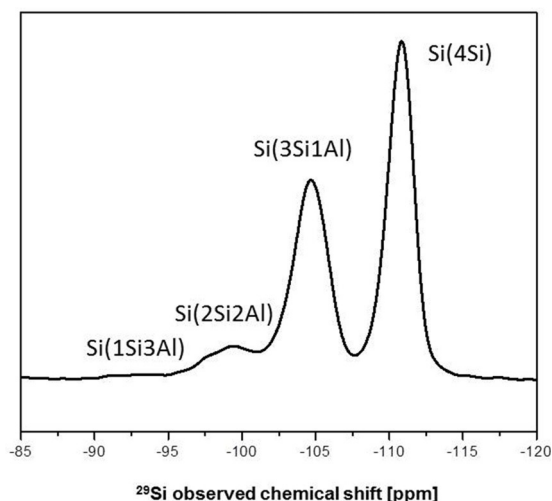


Figure 6. ^{29}Si MAS NMR spectrum of a zeolite with $\text{Si}(n\text{Si},4-n\text{Al})$ atoms ($n=1-4$).

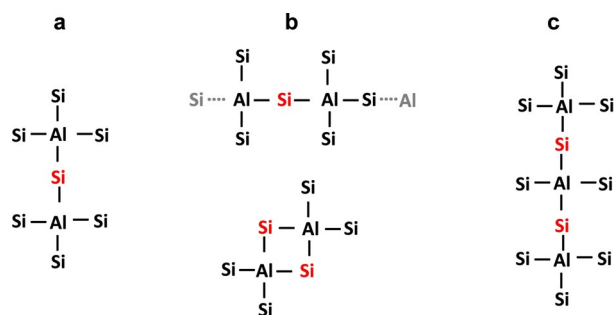


Figure 7. Schematic depiction of AlSiAl a) isolated, b) in ring or infinite chain, and c) in an isolated triad.

in which I_1 is the intensity of the signal corresponding to $\text{Si}(3\text{Si},1\text{Al})$ and I_2 reflects the intensity of the resonances reflecting the $\text{Si}(2\text{Si},2\text{Al})$ atoms (for details, see Ref. [17d]).

Note that this equation is valid only if $\text{Si}(n\text{Si},4-n\text{Al})$ atoms ($n=2-4$) are exclusively present in the zeolite. In the presence of Si atoms with $n < 2$, there is huge variability in the number of possible Al arrangements, which makes even a rough estimate unclear.

The Al arrangement resulting in the lower bound of the concentration of AlSiAl is as follows: $(\text{AlSi})_n$ sequences form an infinite chain or a closed loop (i.e., zeolite ring). In this case, one $\text{Si}(2\text{Si},2\text{Al})$ and two $\text{Si}(1\text{Si},3\text{Al})$ atoms correspond to one Al atom, and the concentration of Al atoms in this Al species is given by Equation (2):

$$\text{Al}_{\text{AlSiAl}} [\%] = \frac{I_2}{(0.5I_2 + 0.25I_1)} \times 100\% \quad (2)$$

A specific case of AlSiAl atoms represents an Al triad. In the case of a triad forming a 6-ring, the concentration of Al atoms is given by Equation (2). In the case of a linear Al triad or a triad in a ring larger than a 6-ring, two $\text{Si}(2\text{Si},2\text{Al})$ and eight $\text{Si}(3\text{Si},1\text{Al})$ atoms belong to three Al atoms. The concentration of Al atoms of such an Al triad is given by Equation (3):

$$\text{Al}_{\text{TRI}} [\%] = \frac{3I_2}{(2.66I_2 + 0.5I_1)} \times 100\% \quad (3)$$

Note that the concentration of Al triads cannot be estimated by using only ^{29}Si MAS NMR spectroscopy, and an additional experiment providing the ion-exchange capacity of the zeolite for divalent metal cation aqua complexes is required. Moreover, Al triads can be analyzed only in zeolites with walls formed by only one layer of $\text{T}(\text{Si},\text{Al})$ framework tetrahedra as it is, for example, in SSZ-13 zeolite, but not in pentasil-ring zeolites with walls formed by a bilayer of $\text{T}(\text{Si},\text{Al})$ tetrahedra. This follows from the fact that their analysis is based on their ability to accommodate only one divalent metal cation aqua complex by three Al atoms, whereas the $(\text{AlSi})_n$ sequence with an even number of n is able to accommodate one divalent metal cation aqua complex by two Al atoms. In the case of zeolites with walls formed by a bilayer of $\text{T}(\text{Si},\text{Al})$ tetrahedra, the Al atoms can face different channels and are, thus, unable to accommodate divalent species.

3.2. Homonuclear correlation ^{27}Al - ^{27}Al MAS NMR spectroscopy for evidence of close Al atoms

This type of ^{27}Al MAS NMR spectroscopy experiment represents the only direct proof of close Al atoms in sequences other than the AlSiAl sequence in zeolite frameworks.^[27] The evidence of close Al atoms is based on so-called correlation experiments. Homonuclear and heteronuclear two-dimensional (2D) MAS NMR spectroscopy correlation experiments provide indications about the atoms that are either close in space (dipolar interaction) or chemically bonded (scalar interaction). Details of this experimental approach are far beyond the scope of this Review; for a deeper introduction to the method, see Refs. [26a,c,28]. In principle, correlation experiments are based on the arrangement of the MAS NMR experiment (pulse sequence), which allows magnetization of one nucleus and its transfer to another nucleus. In the analysis of the vicinity of Al atoms, homonuclear ^{27}Al - ^{27}Al correlation involves transfer of magnetization from one Al atom to a neighboring one.^[27] ^{27}Al is a quadrupolar nucleus, and for a long time a correlation experiment sensitive enough to monitor close Al atoms in Si-rich zeolites was not available. The first successful experiments dealt with the analysis of distances of framework Al atoms bearing Brønsted acid sites and extra-framework Al Lewis sites in dealuminated Al-rich materials.^[29] However, they were also able to indicate close Al atoms in Si-rich materials, such as mordenite and MCM-22 with $\text{Si}/\text{Al} > 8$.^[30] Nevertheless, an ultra-high field spectrometer has to be applied for this purpose. The recently developed ^{27}Al - ^{27}Al double-quantum single-quantum (DQ-SQ) MAS NMR spectroscopy experimental method allows the monitoring of close Al atoms in zeolites with a Si/Al ratio of at least 40 by using a 500 MHz spectrometer, which can be regarded as standard instrumentation in materials research.^[27] Figure 8 shows the ^{27}Al DQ-SQ NMR spectra of ZMS-5 samples containing 15 and 65% Al pairs recorded for various excitation times.

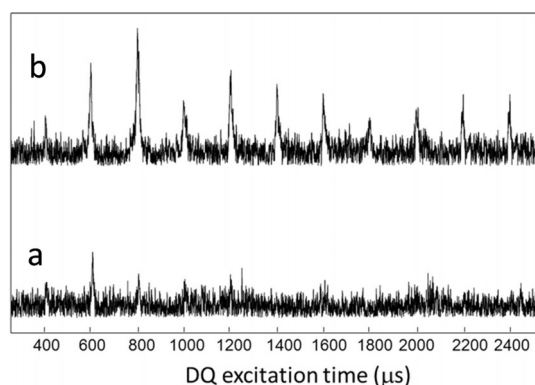


Figure 8. ^{27}Al DQ-SQ NMR spectra of ZMS-5 samples containing a) 15% and b) 65% Al pairs recorded for various excitation times.

Although the ^{27}Al – ^{27}Al DQ-SQ MAS NMR spectroscopy experiment represents a powerful tool for analysis of the organization of Al in zeolite matrices, it suffers from three obstacles. The principal one represents the fact that this correlation experiment cannot distinguish whether the close Al atoms are facing the same channel or not. Thus, it cannot distinguish whether the Al atoms exhibit properties of cooperating Al atoms (Al_{PAIRS} or Al_{CLOSE}) or of isolated ones. Second, the correlation experiment is not yet able to estimate the distances between the Al atoms in Si-rich zeolites, although this can be overcome by rapid progress in this area. Nevertheless, the distances between the Al atoms in different Al species (AlSiAl , Al_{PAIRS} , and Al_{CLOSE}) can be similar, and the correlation experiment is, thus, unable to discriminate between the different Al arrangements. Third, the correlation experiments are not quantitative (similar to all NMR spectroscopy experiments with the exception of single-pulse-type experiments). Thus, they cannot be employed for quantitative analysis of Al species in the framework, and even their application for qualitative comparison of the Al distribution in two different samples is strictly limited. To conclude, the ^{27}Al – ^{27}Al correlation experiment represents an extremely powerful proof of concept and is a tool for the verification of the suggested Al distribution (“whether Al species with close Al atoms are present or not”) or for measuring the Al–Al distances in specific materials and is not a common tool for the analysis of the Al distribution in zeolites.

3.3. ^{27}Al and ^{27}Al MQ MAS NMR spectroscopy for analysis of AlSi_nAl species

^{27}Al multi-quantum (MQ) MAS NMR spectroscopy experiments and recently also ultrahigh-field experiments have enabled Al atoms occupying the individual crystallographically distinguishable T sites to be determined and also allowed their ^{27}Al isotropic chemical shifts (and other NMR parameters as well) to be estimated. It should be noted that Al atoms located in the individual crystallographically distinguishable T sites have very similar local AlO_4^- geometries. This approach is employed for analysis of the Al siting in the individual framework T sites of zeolites with more than one type of crystallographically distinct Al sites in combination with ^{27}Al MAS NMR spectroscopy

for quantitative analysis of the Al siting.^[9b,17a,31] However, different geometries of AlO_4 tetrahedra are caused not only by the Al siting but also by neighboring Al atoms. It has been shown that an Al atom as a next-next-nearest neighbor can change the ^{27}Al isotropic chemical shift up to 4 ppm.^[17a] In the case of zeolites with one crystallographic T site, it has been shown that comparison of the ^{27}Al isotropic chemical shifts of Al atoms in various $\text{AlSi}_{2,3}\text{Al}$ species with their ^{27}Al isotropic chemical shifts predicted by using periodic DFT calculations enables the presence of such species to be excluded or confirmed and also allows their geometrical arrangement in the zeolite framework to be solved.^[16,31a] Figure 9 depicts close unpaired Al atoms in SSZ-13 and their ^{27}Al isotropic chemical shifts.

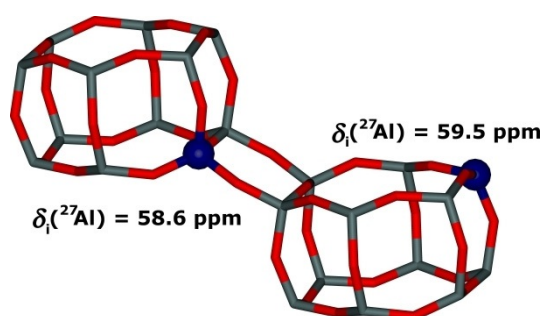


Figure 9. Close unpaired Al atoms in SSZ-13 and their ^{27}Al isotropic chemical shifts.

3.4. Homonuclear correlation ^1H – ^1H and heteronuclear ^1H – ^{27}Al MAS NMR spectroscopy for measurement of the distance of acid sites

^1H – ^1H homonuclear correlation experiments are significantly more sensitive (^1H is not a quadrupolar nucleus) and simpler than ^{27}Al – ^{27}Al measurements.^[26a,c,32] Moreover, this type of experiment gives information on the parameter that is directly connected to catalysis—the distance of the Brønsted acid sites of the bridging AlOHSi groups.^[32,33] Although this experiment does not require specific instrumentation (spectrometers with a ^1H Larmor frequency of 400 MHz seems to be fully sufficient), this type of experiment must be performed on fully dehydrated zeolites. Moreover, similar to ^{27}Al – ^{27}Al correlation experiments, it is not possible to discriminate between protons that can cooperate and protons that are close but unable to cooperate in a catalytic reaction and it is also not possible to quantify the number of close or isolated protonic sites.

In the case of the zeolite beta with a significant fraction of acid sites in the form of framework Al Lewis sites, the ^1H – ^1H correlation does not provide representative information on the distances of the acid sites. We suggest that for this type of catalyst, the ^1H – ^1H experiment should be combined with the ^1H – ^{27}Al heteronuclear experiment (magnetization is transferred from the highly sensitive ^1H nucleus to the ^{27}Al one). This type of experiment has already been applied to characterize the distances of the active sites in dealuminated zeolites, that is, with the Brønsted acid sites of bridging AlOHSi groups and extra-framework Al Lewis sites.^[34]

3.5. M^{2+} cations as probes of Al distribution

In contrast to the above methods that directly investigate Al atoms (or the related acid sites), the following approach is based on the use of divalent transition-metal cations as probes of the Al organization. This approach represents the simplest way to characterize the Al distribution in zeolites. However, from the point of view of acid catalysis, this characterization is highly informative as well and, moreover, allows quantitative analysis.^[8a,10a,18] Note that the transport of M^{2+} aqua complexes inside the zeolite without any restriction is essential for these methods, that is, a well-calcined zeolite without trace amounts of template, with the absence of extra-framework Al and Si species, and without silylation of the zeolite crystals.

3.6. Monitoring of single Al atoms by the maximum M^{2+} ion-exchange capacity

3.6.1. Co^{2+} ion exchange

Single Al atoms are defined as Al atoms that are so far away that they are not able to accommodate a Co^{2+} hexaaqua complex. Thus, the maximum ion-exchange capacity of a zeolite for the Co^{2+} hexaaqua complex can be used as a measure of the single Al atoms according to Equation (4):

$$[Al_{SINGLE}] = [Al_{FR}] - 2 [Co_{MAX}] \quad (4)$$

in which $[Al_{FR}]$ is the framework Al content and $[Co_{MAX}]$ is the maximum Co^{2+} hexaaqua complex ion-exchange capacity of the zeolite.^[8a,10a,18] To guarantee that maximum ion exchange is reached, ion exchange to the sodium form of the investigated zeolite must be performed three times for 24 h. To guarantee the exclusive presence of the Co^{2+} hexaaqua complex in the ion-exchange solution, a maximum solution concentration of 0.05 M is recommended, along with ambient temperature and Co nitrate as the Co^{2+} source. Note that these conditions prevent hydrolysis of the Co^{2+} hexaaqua complex. The parent zeolite in the Na form guarantees fast ion exchange and, moreover, enables simple estimation of the total charge balance of the Co-exchanged zeolite $[(2Co+Na)/Al]$, which should be close to unity.

In general, other divalent cations can also be employed to monitor the Al distribution. However, Vis spectroscopy allows simple monitoring of the exclusive presence of the Co^{2+} hexaaqua complex both in the ion-exchange solution and in the Co^{2+} -exchanged zeolite. The spectrum of the Co^{2+} hexaaqua complex is well known, and all perturbations related to Co^{2+} cation coordination are simply detectable as new bands with extinction coefficients that are significantly higher than those of the bands of the Co^{2+} hexaaqua complex (its d-d transitions are symmetrically forbidden, and breaking of the octahedral symmetry of the Co^{2+} hexaaqua complex makes d-d transitions symmetry allowed).^[35] Figure 10 shows the Vis spectrum of hydrated ZSM-5 ion exchanged by Co nitrate.

In hydrated zeolites and under the conditions of ion exchange of a solvated divalent complex, the location of both Al

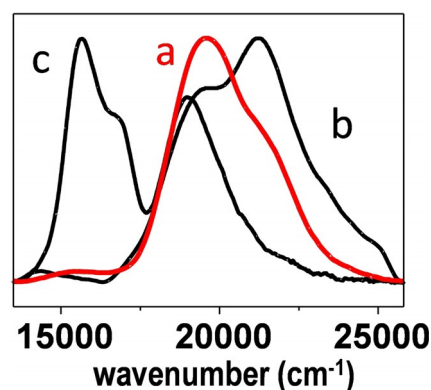


Figure 10. Vis spectrum of hydrated ZSM-5 a) ion exchanged by Co nitrate with the exclusive presence of Co^{2+} hexaaqua complexes and ion exchanged by Co acetate b) at RT and c) at 80 °C with Co^{2+} species exhibiting perturbed octahedral coordination.

atoms in one ring is not decisive, and the ion-exchange capacity is controlled by the “functional” distance (in one ring/cavity) of the Al atoms. In the case of dehydrated zeolites, the stabilization energy of bare M^{2+} cations is significantly affected by the location of the Al atoms in one or two rings.^[20] In the latter case, the stabilization energy of a bare M^{2+} cation coordinated only to one AlO_4 tetrahedron is low, and the cation in such a site is supposedly highly reactive. This results in the formation of Co-oxo species ($[Co^{2+}OH]^-$ or $[Co^{3+}O^{2-}]^-$) during dehydration of the hydrated sample (depending on the conditions of dehydration).^[15,17d,19,21] Thus, the discrimination of Co-oxo species from bare Co^{2+} cations and quantitative analysis of bare Co^{2+} cations in the maximum Co-exchanged dehydrated zeolites represent key issues of this method. There is no universal method for this. Several approaches have been developed, and each exhibits its own strong and weak points that have to be taken into account. The concentration of Al atoms in Al pairs is then given by Equation (5)^[10a,15,18] and that of close unpaired Al atoms is given by Equation (6).^[15,17d,19,21]

$$[Al_{PAIRS}] = 2 [Co_{BARE}] \quad (5)$$

$$[Al_{CLOSE}] = 2 ([Co_{MAX}] - [Co_{BARE}]) \quad (6)$$

in which $[Co_{BARE}]$ is the concentration of bare Co^{2+} cations in the dehydrated maximum Co-exchanged zeolite.

3.6.2. Cu^{2+} ion exchange

Exchange of the Cu^{2+} hexaaqua complex represents an analogy to the ion exchange of the Co^{2+} hexaaqua complex.^[36] However, Cu^{2+} complexes are, according to our experience, significantly more sensitive to the conditions both in the ion-exchange solution and inside the channels of hydrated zeolites. Thus, the pH of the solution has to be carefully tuned during the ion-exchange process. Moreover, although the spectra of Cu^{2+} aqua complexes reflect deviation from the octahedral symmetry, the change in the symmetry following hydrolysis of the Cu^{2+} hexaaqua complex is reflected, in contrast

to the Co^{2+} complexes, only by a not-well-pronounced shift in the band edge to higher wavenumbers.^[35,37]

3.7. Adsorption of $[\text{D}_3]$ acetonitrile on dehydrated Co-zeolite

A bare Co^{2+} cation in a cationic site of a dehydrated zeolite is an acceptor of an electron pair and behaves as a Lewis acid site. Thus, adsorption of probe molecules with base properties, as monitored by FTIR spectroscopy, represents a suitable tool for the quantitative analysis of bare Co^{2+} sites. Although one of the most used molecules for monitoring Brønsted and Lewis sites in zeolites is pyridine, $[\text{D}_3]$ acetonitrile can also be used, because, in contrast to pyridine, it is able to go through 8-rings and to penetrate into the channels/cavities of all zeolites (with some exceptions, see below). The advantage of this method is simple analysis of the IR spectrum of $[\text{D}_3]$ acetonitrile adsorbed in a dehydrated Co-zeolite. The concentration of Al in Al pairs is then given by Equation (7), and the concentration of close unpaired Al atoms is given by Equation (8):^[17d,19,21,24]

$$[\text{Al}_{\text{PAIR}}] = 2 [\text{Co}_{\text{LEWIS}}] \quad (7)$$

$$[\text{Al}_{\text{CLOSE}}] = 2 ([\text{Co}_{\text{MAX}}] - [\text{Co}_{\text{LEWIS}}]) \quad (8)$$

in which $[\text{Co}_{\text{LEWIS}}]$ represents the concentration of bare Co^{2+} cations adsorbing $[\text{D}_3]$ acetonitrile. Important for this method is to guarantee that $[\text{D}_3]$ acetonitrile is adsorbed on all of the bare Co^{2+} cations and, moreover, that only one $[\text{D}_3]$ acetonitrile molecule is adsorbed on one Co cation. The first requirement can be proven by inspection of the antisymmetric Co^{2+} -related T–O–T vibrations (see next paragraph), which have to disappear. The second requirement can be proven by finding the conditions of desorption (time, temperature) under which Co^{2+} cations related to T–O–T vibrations start to reappear. It has to be taken into account that $[\text{D}_3]$ acetonitrile is not able to penetrate through 6-rings. Thus, bare Co^{2+} cations in sites with access strictly limited by such rings, for example, the sites inside the hexagonal prism of FAU or CHA structures or inside the cages of FAU or *BEA (the α and γ sites of the beta zeolite)^[15,17d,38] are not reflected in the adsorption of $[\text{D}_3]$ acetonitrile. Nevertheless, this represents an advantage in redox reactions,

as although these sites accommodate bare divalent cations, these cations are inaccessible and cannot act as an active site. In protonic forms, the related acid sites face different channels/cavities and represents single acid sites, not sites related to close unpaired Al atoms. This might require a correction according to Equation (9); however, the concentration of this type of cationic site is rather low.

$$[\text{Al}_{\text{SINGLE}}] = [\text{Al}_{\text{FR}}] - 2 ([\text{Co}_{\text{MAX}}] - [\text{Co}_x]) \approx [\text{Al}_{\text{FR}}] - 2 [\text{Co}_{\text{MAX}}] \quad (9)$$

in which $[\text{Co}_x]$ ($x = \alpha$ in beta zeolite, γ , D6R) is the concentration of bare Co^{2+} cations in the inaccessible cage obtained from other methods (see below).

A significantly more important obstacle of this method originates from the fact that rings forming some cationic sites (the β site in ferrierite and mordenite) in certain zeolites face a significantly restricted channel/pocket. In this case, a high concentration of Al pairs in these rings can result in steric hindrance for the adsorption of $[\text{D}_3]$ acetonitrile to each Co^{2+} cation located in these rings and, thus, in underestimation of the concentration of bare Co^{2+} cations in the zeolite. Figure 11 shows the FTIR spectrum of $[\text{D}_3]$ acetonitrile adsorbed on the dehydrated TNU-9 zeolite and the effect of the Co loading on adsorption of acetonitrile in TNU-9 and beta zeolites.

3.8. Perturbations of antisymmetric T–O–T vibrations of dehydrated Co-zeolites

Coordination of bare divalent cations to the oxygen atoms of the AlO_4 tetrahedra of the zeolite ring-forming cationic sites results in deformation of the ring and perturbation of the related T–O–T vibrations.^[15,16,18,39] This is a consequence of the flexibility of the zeolite framework, on the one hand, and the strictly preferred Co–O distance close to 2 Å, on the other hand.^[39d,e,40] In some zeolites, these perturbed T–O–T vibrations are shifted to the window of T–O–T vibrations (exhibiting a low intensity of all other skeletal vibrations) and can be monitored by FTIR spectroscopy. Although the characteristic T–O–T vibrations reflecting M^{2+} siting in individual sites can be distinguished, their extinction coefficients are highly similar.^[15] Thus, the total intensity of all Co^{2+} -related T–O–T vibrations can serve as a

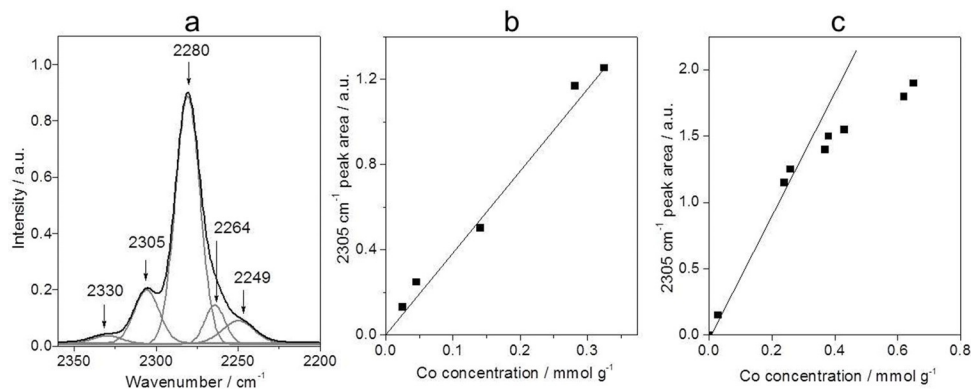


Figure 11. a) FTIR spectrum of $[\text{D}_3]$ acetonitrile adsorbed on dehydrated TNU-9 and the effect of Co loading on acetonitrile adsorption in b) TNU-9 and c) beta zeolite. Assignment of the bands: Al_{FR} : 2330 cm^{-1} , Co^{II} Lewis sites: 2305 cm^{-1} , Na^+ : 2280 cm^{-1} , SiOH : 2264 cm^{-1} , physisorbed CD_3CN : 2249 cm^{-1} .

measure of the total concentration of bare Co^{2+} cations and, thus, the total concentration of Al pairs; hence, it can also be employed to analyze the Co^{2+} siting and the location of Al pairs in the individual rings/cationic sites. This represents a significant advantage over the adsorption of $[\text{D}_3]\text{acetonitrile}$. Moreover, this approach is not affected by the accessibility of the cationic sites or by spatial restrictions in the adsorption of probe molecule. Further, divalent cations with adsorbed probe molecules or impurities can be easily identified. The concentration of Al in Al pairs is then given by Equation (10), and the concentration of close unpaired Al atoms is given by Equation (11):

$$[\text{Al}_{\text{PAIR}}] = 2 \sum [\text{Co}_\chi^{\text{TOT}}] \approx 2 [\text{Co}^{\text{TOT}}] \quad (10)$$

$$[\text{Al}_{\text{CLOSE}}] = 2 ([\text{Co}_{\text{MAX}}] - [\text{Co}^{\text{TOT}}]) \quad (11)$$

in which $[\text{Co}^{\text{TOT}}]$ is the concentration of bare Co^{2+} cations from the total intensity of the perturbed T–O–T vibrations and $[\text{Co}_\chi^{\text{TOT}}]$ is the concentration of bare Co^{2+} cations in the individual cationic site χ formed by the Al pair (not the site of the cation in a cage) from the intensity of the corresponding T–O–T vibrations. The concentration of Co cations in a cage can be used as a correction for $[\text{Co}_\chi]$ in Equation (8). Also, other divalent cations can be used with this method. However, the frequencies of perturbed T–O–T vibrations related to bare M^{2+} cations have been reported predominantly for Co-zeolites, and the ion exchange of Co cations to the zeolite is robust and easily monitored. The main obstacle associated with this approach is the quality of the window in the region of the anti-symmetric T–O–T vibrations, which depends on the topology of the zeolite (excellent for ferrierite; good for ZSM-5 the beta zeolite, TNU-9, and SSZ-13) and on the crystallinity of the sample.^[15, 16, 24, 39a, b, h, 40, 41] Figure 12 shows the effect of Co^{2+} coordination on the geometry of the zeolite 6-ring, the FTIR spectrum of dehydrated Co-TNU-9 in the region of T–O–T vibrations with simulation of the spectrum to the individual bands, and the effect of Co loading in TNU-9 on the total intensity of the T–O–T vibrations.

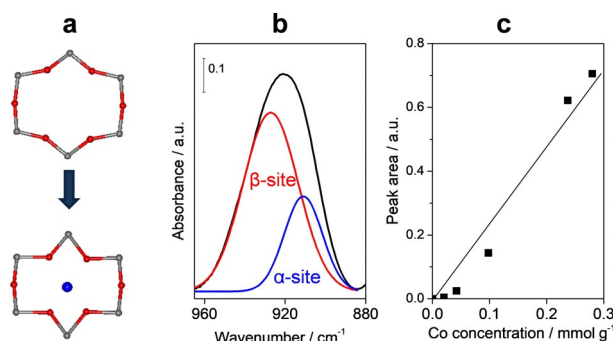


Figure 12. a) Effect of Co^{2+} coordination on the geometry of the zeolite ring, b) FTIR spectrum of dehydrated Co-TNU-9 in the region of T–O–T vibrations with simulation of the spectrum to the individual bands, and c) effect of Co loading in TNU-9 on the total intensity of the T–O–T vibrations.

3.9. Vis spectra of Co^{2+} d–d transitions in dehydrated zeolite

Bare Co^{2+} cations located in cationic sites of zeolites exhibit d–d transitions that are present in the Vis region of the spectrum of dehydrated Co-zeolites. These transitions are complex but sensitive to the coordination of bare Co^{2+} cations. In contrast to T–O–T vibrations, the extinction coefficients in the individual sites can significantly differ. Thus, analysis of Al pairs in the zeolite first requires detailed analysis of the spectrum of the dehydrated Co-zeolite, including identification of spectroscopic species corresponding to the base Co^{2+} cations (one to four bands have been reported to reflect one coordination of Co^{2+} cations) and estimation of the corresponding extinction coefficients. Nevertheless, for several zeolites this analysis has been done and reported (mordenite, ferrierite, ZSM-5, the zeolite beta, and SSZ-13).^[15, 24, 39c, 42] The concentration of Al in Al pairs is then given by Equation (12), and the concentration of close unpaired Al atoms is given by Equation (13).^[8a, 10a, 18]

$$[\text{Al}_{\text{PAIR}}] = 2 \sum [\text{Co}_\chi^{\text{dd}}] \quad (12)$$

$$[\text{Al}_{\text{CLOSE}}] = 2 ([\text{Co}_{\text{MAX}}] - \sum [\text{Co}_\chi^{\text{dd}}]) \quad (13)$$

in which $[\text{Co}_\chi^{\text{dd}}]$ is the concentration of bare Co^{2+} cations in the individual cationic site formed by the Al pair from the Co^{2+} d–d transitions. In analogy to the approach based on the T–O–T vibrations, the d–d transitions also reflect Co^{2+} cations located in inaccessible sites in prisms or cages. The main disadvantages of this method are difficult analysis of the spectrum, the necessity to identify the spectroscopic species and the extinction coefficients, and the risk of the adsorption of impurities (water molecules) on the bare Co^{2+} cations (the presence of water in the sample can be monitored only by UV/Vis-near-IR spectrometers). Conversely, this approach is necessary to identify the cation and, thus, the Al pair siting. Figure 13 depicts the cationic sites and corresponding Vis spectra of Co cations in a ZSM-5 zeolite.

3.10. Theoretical approaches based on minimization of energies

As shown in the next sections, the Al distribution in the zeolite is governed by the conditions used to synthesize the zeolite. Moreover, zeolites do not represent a thermodynamically stable system, as follows from the effects of temperature on the synthesis of zeolite that indicate that formation of the zeolite matrix is also affected by kinetics. Thus, the suggestion that Al is organized in the zeolite framework on the basis of a minimization of the lattice energy or even on a minimization of the energy of the cations in individual cationic sites in dehydrated zeolites formed by different Al arrangements in the framework does not represent a reasonable approach for the analysis of the Al distribution in the zeolite framework, unless all the conditions of the synthesis [the presence of water, structure-directing agents (SDAs), inorganic cations, pH, temperature, pressure, Al and Si species present in the synthesis

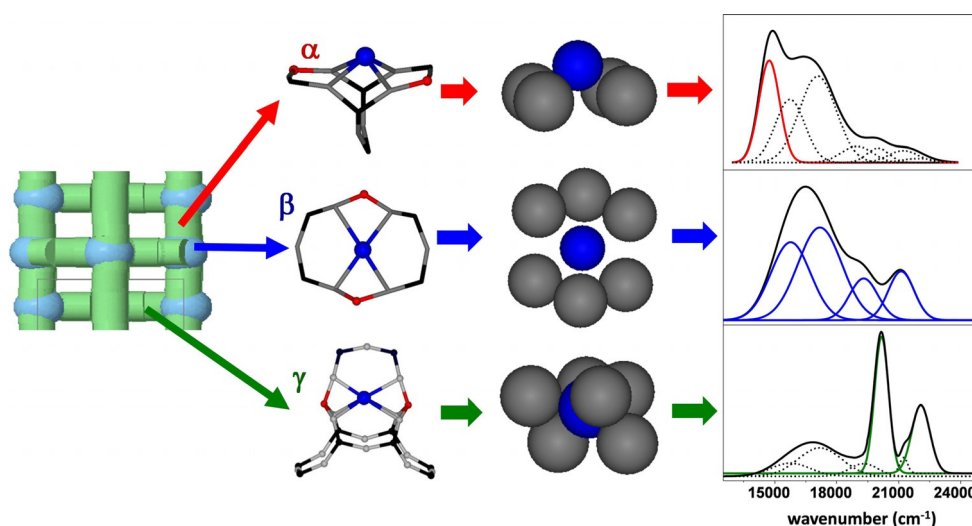


Figure 13. Cationic sites and corresponding Vis spectra of Co cations in a ZSM-5 zeolite.

gel] are included in the calculation. Without that, the calculated stabilization energies of the Al atoms in the framework T(Al) sites or in individual SiAl species represent maximally a measure of the stability of the individual Al species against dealumination or a rough tool to predict if the zeolite with the suggested Al organization can exist after removal of organic SDA. The calculated stabilization energies of cations in the cationic sites in dependence of the organization of Al in the framework can serve only to predict the preferences of the cations in the sites if the sites are really present in the zeolite framework, that is, if the zeolite framework has Al atoms (i.e., Al pairs) that form these sites.

4. Variability of the Al Distribution in Zeolites

There is only one type of Al distribution in zeolites that has never been observed, and it is the Al–O–Al sequence. Its absence in aluminosilicate materials, in general, has resulted in the formulation of the “Loewenstein rule”.^[13] The fact that two zeolites of the same topology and chemical composition can exhibit markedly different Al distributions clearly suggests that the Al distribution in zeolites is not random or controlled by some statistical rules but depends on the conditions of the synthesis of the zeolites.^[8a,11,43] This clearly dispels the “Dempsey rule”, which suggests that the stabilization energy of the Al–O–Si–O–Al sequence in zeolites governs their occurrence,^[44] and the “Takaishi and Kato rule”, which forbids the presence of two Al atoms in a 5-ring.^[45] Thus, there are no rules other than the “Loewenstein rule” to determine the organization of Al in the framework of zeolites, and with the exception of Al–O–Al species, all other possible types of Al organizations have already been reported for Si-rich zeolites. State-of-art knowledge regarding the Al distribution in different zeolite matrices is summarized below.

4.1. ZSM-5

ZSM-5 is one of the most important zeolites in the field of catalysis and attracts enormous attention. Moreover, its synthesis is rather robust, and zeolites of the MFI topology can be prepared by many different routes. This results in enormous variability in the Al distribution in this zeolite, and it is possible to prepare zeolites with highly variable Al distributions between single Al atoms and Al pairs over practically the whole range of framework Al contents, which is typically Si/Al = 12 to ∞ .^[8a,10a,11a,12,15,38,43] It is even possible to prepare ZSM-5 zeolites with a semi-monomodal Al distribution (with more than 90% Al in one type of Al species) in the Si/Al range of 14 to 60.^[12,44] AlSiAl sequences have not been reported for ZSM-5 samples with Si/Al > 10.^[8a] Conversely, the Al atoms in Al-rich ZSM-5 samples with Si/Al < 10 are predominantly present in the form of AlSiAl sequences. Al atoms of these sequences face different channels, and thus, these Al atoms exhibit the behavior of isolated Al atoms from a catalysis point of view.^[8a,17a] In contrast to laboratory samples, the Al distribution in commercial ZSM-5 zeolites is not more variable, and single Al atoms prevail over the entire range of contents of framework Al. Only a small increase in the concentration of Al pairs is observed for available commercial samples at the lowest Si/Al ratio (Si/Al < 18).^[12,38]

Al pairs in ZSM-5 are located in three cationic sites, designated as α , β , and γ sites. The α and β sites represent 6-rings on the channel walls (α site in the main channel, β site at the channel intersection).^[39c] The so-called boat-shaped γ site is rather complex, and the exact arrangements of the Al atoms and bare divalent cations are unclear. Al pairs in β sites significantly prevail and represent at least 50% of the Al pairs in the samples in the entire Si/Al region. Al pairs in α sites do not exceed 35% of Al in pairs, and the Al concentration in the γ sites is negligible.^[11a,39c,43] Knowledge of the locations of Al pairs in cationic sites allows the location of Al in samples with predominating Al pairs to be analyzed. Al pairs in the β site

are located in the ZSM-5 intersection. In the case of the α site, the site itself (or cations located in this site) faces the main ZSM-5 channel, but the Al atoms of the Al pairs in this site are each located at the edge of one channel intersection. Thus, the Al atoms in samples with predominating Al pairs (all of them prepared by using tetraalkylammonium cations as organic SDAs) are associated with the intersection of ZSM-5 channels. Moreover, isolated Al atoms in ZSM-5 samples with prevailing single Al atoms (prepared by using tetraalkylammonium cations as organic SDAs) are also mainly located at the channel intersection. It can be concluded that in ZSM-5 zeolites synthesized by using tetraalkylammonium cations as organic SDAs the Al atoms are located at the channel intersection without relation to the distribution of Al.^[12,46] Figure 14 reveals the Al distribution in ZSM-5 and a schematic representation of the locations of single Al atoms and Al pairs.

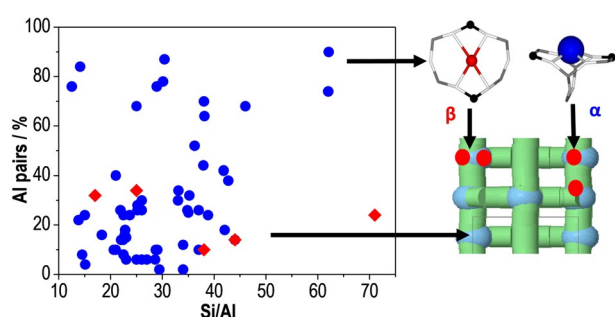


Figure 14. Al distribution in ZSM-5 and schematic representation of the location of single Al atoms and Al pairs. Laboratory (●) and commercial syntheses (◆).

4.2. Beta zeolite

Beta zeolite has also attracted significant attention, as this structure represents the only Si-rich (but Al-containing) large-pore zeolite with a 3D channel system. In discussing the Al distribution in beta zeolite with large pores, it is necessary to keep in mind that significant dealumination can occur in these zeolites during removal of the high concentrations of organic SDAs needed for their synthesis. Thus, samples could be partially dealuminated. Nevertheless, tetramethylammonium cations can be removed in a stream of ammonia without perturbing the framework. The synthesis of beta zeolites with a low concentration of tetramethylammonium (using the seed ap-

proach) cations provides unperturbed zeolites as well. This allows characterization of the Al organization in the unperturbed framework of the beta zeolite. Unperturbed Si-rich zeolites ($\text{Si}/\text{Al} > 10$) of the BEA topology are free of AlSiAl sequences. The concentration of Al pairs can vary between 40 and 65% of the Al atoms (for $\text{Si}/\text{Al} < 18$). However, in contrast to ZSM-5 and other pentasil-ring zeolites, the rest of the Al atoms in unperturbed beta samples with $\text{Si}/\text{Al} < 18$ do not represent single Al atoms, but instead represent close unpaired Al atoms.^[19,21] This type of Al atom is, to the best of our knowledge, unique (with the exception of the recently reported SSZ-13 zeolite^[16]) to beta zeolites.

Al pairs in beta zeolites form three cationic sites, designated as α , β , and γ sites, with local arrangements similar to those observed in the ZSM-5 zeolite. Also, their populations (β sites at least 50%, α sites less than 35% of the Al in pairs, and Al in γ sites is negligible) are similar.^[15] Nevertheless, there is a substantial difference in the relation of the cationic sites (Al pairs) to the zeolite channel system. In contrast to the ZSM-5 zeolite, not only divalent cations in the γ sites but also those accommodated in the 6-ring of the α sites are not accessible to guest molecules, as the divalent cations are located inside the beta cage and are not reflected in the adsorption of $[\text{D}_3]\text{acetonitrile}$.^[38] Therefore, their role in catalytic reactions is most likely negligible. In the case of acid sites related to framework Al forming these two cationic sites, that is, framework Al Lewis sites (which can represent up to 60% of the acid sites in beta zeolite)^[47] and Brønsted protonic sites, they face different channels and cannot cooperate regardless of their type. Only the Al atoms of the 6-ring of the β site face the same channel and can cooperate, and cations in this site are accessible to the reactants.

In the case of Al-rich beta zeolites ($\text{Si}/\text{Al} = 4.5\text{--}6$), Al in the AlSiAl sequences predominates and represents at least 60–80% (the lower bound) of the Al atoms. These AlSiAl sequences are arranged across the zeolite walls and face different channels without any manifestation of their presence as close acid sites or as cationic sites for divalent cations. Close unpaired Al atoms represent up to 80% of the Al atoms on the channels' surface, whereas Al pairs represent a maximum 30% of the Al atoms at the channel surface in Al-rich beta zeolites.^[17d,41a] Recently, post-synthetic modification of boron beta zeolite has been developed to prepare beta zeolites containing exclusively single Al atoms. Figure 15 depicts the schematic representation of Al siting in beta zeolites.^[15,17d]

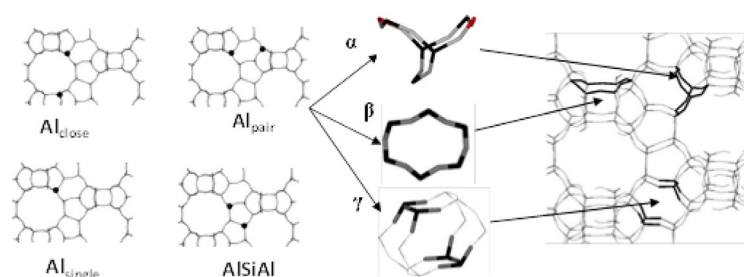


Figure 15. Schematic representation of Al sitings in beta zeolites.

4.3. SSZ-13

SSZ-13 has recently emerged as a material from industry, and it shows enormous potential in catalysis (i.e., in NO_x abatement from diesel exhausts) as the first available Si-rich small-pore zeolite. Catalytic results indicate variability in the Al distribution.^[36b,48] Tuning of the Al distribution by varying the SDA and the Al source results in dramatic variation in the content of single Al atoms in the zeolite (Si/Al = 14–18). Nevertheless, detailed analysis of the Al distribution was not performed^[49] until recently.^[16] Detailed analysis has shown that tuning the synthesis properties results in samples with a semi-modal distribution with single Al atoms (75–90% of Al for Si/Al = 9–13) or a high concentration of close unpaired Al atoms (54% for Si/Al = 12).^[16,17c] It has to be pointed out that this type of Al arrangement is known only for beta zeolites. Conversely, the Al atoms in Al pairs do not exceed 25% of Al for samples below Si/Al = 13. These Al pairs are formed by both AlSi₂Al and AlSi₃Al sequences (the only zeolite proven to have AlSi₃Al pairs) and form three cationic sites: σ sites of the 6-ring with two Al atoms in the AlSi₂Al pair and τ^{2Si} and τ^{3Si} sites formed by AlSi_{2,3}Al pairs located in the 8-ring. Moreover, ω sites are formed by the AlSi₂Al sequence with each Al atom in a different 6-ring. Note that cations in these ω sites are not accessible to the reactants, and the related acid sites are separated and face different cavities. For Al-rich SSZ-13 samples (Si/Al < 7), AlSiAl sequences (similar to Al-rich beta zeolite and ZSM-5) are typically dominant. AlSiAl sequences have also been reported for SSZ-13 samples with Si/Al > 11.^[50] In contrast to pentasil-ring zeolites, the Al atoms of AlSiAl sequences cannot be separated by zeolite walls, and the related monovalent centers can cooperate. For some Al-rich samples prepared from A and X zeolites, a unique Al organization has been reported. Al atoms in Al triads (AlSiAlSiAl sequences) forming the 6-ring represent a significant fraction of the Al atoms (> 50%) in these samples.^[17c] Although they are formed by neighboring Al atoms and face the same cavity, their capacity to accommodate divalent species is low, that is, only one divalent cation per three Al atoms. However, the acid sites related to them are very close and can cooperate. Figure 16 reveals the siting of Al pairs and close unpaired Al atoms in SSZ-13.

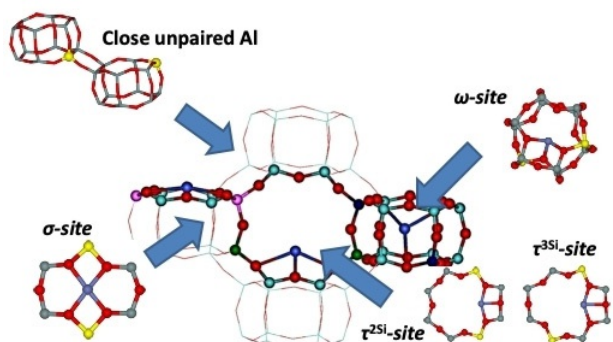


Figure 16. Siting of Al pairs and close unpaired Al atoms in SSZ-13.

4.4. Ferrierite

Ferrierite is a pentasil-ring zeolite that is applied in industry, and its channel system is formed by a combination of 10-ring channels and 8-ring channels. Samples with various Al distributions have been prepared for Si/Al \approx 10. Samples with Al pairs representing between 65 and 12% of Al in pairs and 35 and 88% of single Al atoms have been reported.^[8a,42b] AlSiAl sequences have not been reported for ferrierites with Si/Al > 7.5, and close unpaired Al atoms are not known for this type of framework.^[8a] In samples with Si/Al > 20, single Al atoms predominate and represent 75–95% of the Al atoms.^[31a] The α , β , and γ cationic sites exhibit arrangements similar to those in ZSM-5 (two types of 6-rings and a boat-shaped site). Al pairs in β sites predominate (60% of Al pairs), and this is followed by Al pairs in α sites, which make up a maximum of 35% of the Al pairs in Al pair-rich samples.^[42b] A unique feature not reported for any other zeolite is a “superstructure” of four Al atoms of two Al pairs in two opposite rings of the β sites.^[8a,23] Figure 17 shows Al pairs located in ferrierite^[8a,31a] and mordenite.^[8a,42a]

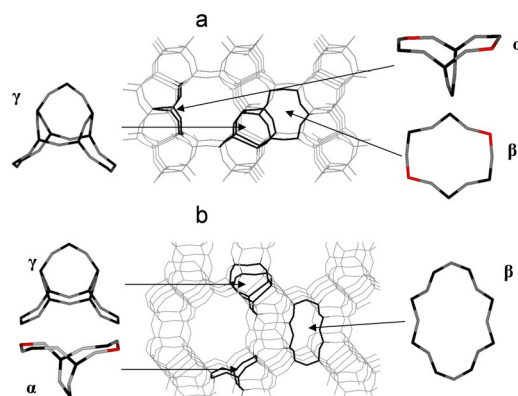


Figure 17. Al pair sitings in a) ferrierite and b) mordenite.

4.5. Mordenite

After beta zeolite, mordenite is the second largest pore pentasil-ring zeolite with Al in the framework and a mono-dimensional channel system formed by 12 ring channels and side pockets that are accessible through 8-rings. It is possible to prepare samples with 44–62% Al in pairs and 56–38% single Al atoms for Si/Al \approx 8.^[8a,42a] For the sample with Si/Al = 5.5, 35% Al atoms in Al pairs ($Co_{MAX}/Al = 0.17$) and 65% single Al atoms are observed. Nevertheless, a significant fraction of Al atoms in the AlSiAl sequence (> 60%) is present in this sample.^[8a,42a] The discrepancy between a low Co^{II} ion-exchange capacity and a high population of AlSiAl sequences indicates that, similar to the above-reported Al-rich beta zeolites, AlSiAl sequences in Al-rich mordenite are arranged across the zeolite wall. Thus, the related acid sites exhibit single Al atom behavior. Close unpaired Al atoms have not been reported for the mordenite topology. Al pairs in mordenites form three cationic sites, α , β , and γ . The arrangement of the α and γ sites located in the

main channel and the mordenite pocket is practically identical to that in ferrierite. Nevertheless, the β sites, which are located at the mordenite pocket and predominate (> 60% of Al pairs), are formed by an 8-ring and can correspond to either AlSi_2Al or AlSi_3Al pairs.

4.6. MCM-22

MCM-22 is a pentasil-ring zeolite with a complex channel system formed by very large cavities open to the external surface or interconnected by 10-ring channels. Al contents from 18 to 68% in Al pairs and from 82 to 32% in single Al atoms have been reported for MCM-22 samples with Si/Al ratios ranging from 25 to 40. For Si/Al = 18, the Al pairs can vary between 36 and 72%.^[8a] Close unpaired Al atoms as well as AlSiAl sequences have not been reported for MCM-22 materials.

4.7. TNU-9

TNU-9 is a 10-ring channel pentasil-ring zeolite, and its channel system, size, and arrangements are similar to those of ZSM-5 but are significantly more complex. There is no information on the variability of the Al distribution, as the organization of Al has been analyzed for only one sample. Single Al atoms represent 40% and Al in Al pairs represent 60% of all the Al atoms for Si/Al = 14. AlSiAl sequences and close unpaired Al atoms are not observed.^[24] The Al pairs form three cationic sites, α , β , and γ , and they are highly similar to those in ZSM-5. The only one substantial difference is that the concentration of Al pairs in the γ site is negligible. The β sites of the 6-ring at the channel intersection represent 85% of Al pairs (50% of total Al), and for the α sites in the channel with the Al atoms belonging to two intersections, the value is only 15% of the Al pairs. At least 60% of Al has, thus, been suggested to be located at the TNU-9 intersection. Therefore, from the point of view of the Al distribution, TNU-9 can be regarded as analogous to those laboratory-prepared ZSM-5 zeolites, which are rich in Al pairs.

5. Tuning the Al Distribution

The above-described variability in the Al distribution in zeolites with similar framework Al contents clearly evidences that the Al distribution in zeolite frameworks is not random or controlled by some simple rules (including thermodynamics of the framework), but it has to depend on the conditions used for zeolite synthesis. This brings up the question as to how the synthesis can be tuned to govern the Al distribution to optimize the properties of zeolite catalysts. The mechanism for the synthesis of zeolites is out of the scope of this review. Moreover, it has to be pointed out that tuning the Al distribution in zeolite synthesis, as a starting point, involves the successful synthesis of the zeolite, and thus, the synthesis parameters can only be manipulated slightly. For the purpose of tuning the Al distribution in zeolites, it has to be noted that the building of zeolite frameworks is a result of the interplay among the (organic) structure-directing agent, other cations balancing the negative charge of the formed framework, and the Al and Si

sources used to build the framework (the main partners in the formation of the synthesis gel). The effects of the individual partners of the synthesis and mechanisms affecting the Al distribution have recently been studied in detail for ZSM-5. The authors focus their attention on the synthesis by using a "dense" gel analogous to the conditions used in industrial synthesis, whereas they exclude the use of clear gels and seeds. Note that the formation of close Al atoms has not yet been studied.

5.1. Polarization of the SDA (variation of the Al source)

Polarization of the SDA cation in the synthesis mixture has been suggested to affect the formation of single Al atoms and Al pairs. The SDA^+ plays two roles in the synthesis process. It organizes various types of (alumino)silicate species to form a complex framework with a defined channel system and balances the negative charge of AlO_4^- tetrahedra in the framework. A high polarization of SDA^+ by OH^- present in the basic synthesis mixture results in the highest probability that SDA^+ cations are able to balance two close negative charges connected with two AlO_4^- anions to form an AlSi_2Al sequence. A decrease in the polarization of SDA^+ by replacement of OH^- by less-polarizing anions results in an increase in the fraction of isolated Al atoms in the framework, as less-polarized SDA^+ balances only one AlO_4^- tetrahedron. Replacement of OH^- by Cl^- decreases the concentration of Al pairs to one half, and replacement of OH^- by NO_3^- decreases the concentration of Al pairs even to less than one sixth of their original concentration. The simplest way to change the polarization of SDA^+ without changing the other parameters of the synthesis is to vary the Al source and to replace metallic Al or $\text{Al}(\text{OH})_3$ by various Al salts. The following polarization effect has been suggested: $\text{OH}^- > \text{Cl}^- \approx \text{PO}_4^{3-} > \text{NO}_3^-$.^[11a,43] It can be speculated that the effect of different SDAs on the Al distribution in ZSM-5 can also be explained by this mechanism.^[51]

5.2. The presence of an inorganic co-cation in the synthesis mixture

In the growing zeolite framework, AlO_4^- tetrahedra can be balanced not only by SDA^+ but also by other cations such as Na^+ . The addition of Na^+ from various salts results in the synthesis of Si-rich matrices with a significant increase in single Al atoms compared to the synthesis without added Na^+ . Note that a synergistic effect of the polarization of the SDA^+ can be reached if a properly selected sodium salt is used. It has to be pointed out that for zeolites with a higher number of crystallographically distinguishable framework T sites, the addition of Na^+ to the synthesis mixture results in a wider dispersion of Al atoms in these sites. In the synthesis for which only SDA^+ cations are used, Al atoms are located in the vicinity of the cationic part of the SDA^+ molecules (e.g., N atom in tetraalkylammonium cations), whereas the presence of significantly smaller Na^+ cations also allows the Al atoms to be balanced in other T positions. In the synthesis of Al-rich materials (e.g., ZSM-5 with Si/Al < 20) for which the presence of Na in the synthesis mix-

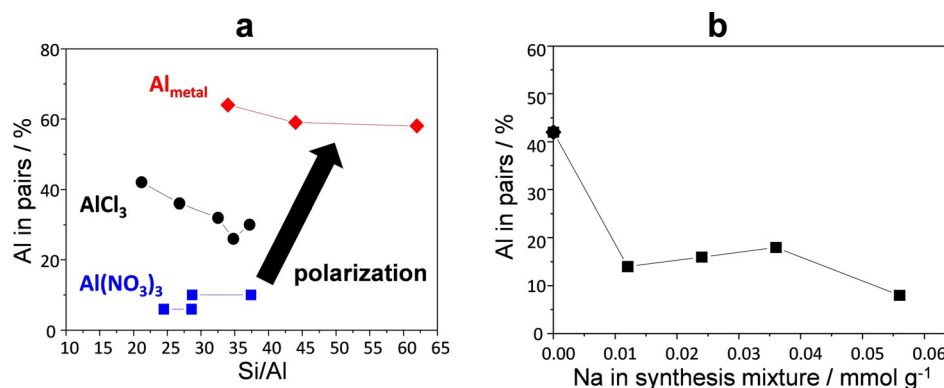


Figure 18. Effects of a) the polarization (i.e., of the Al source) and b) the addition of NaCl on the Al distribution in ZSM-5 synthesized by using TEOS as the Si source and TPAOH as the SDA.

ture is required, the Na⁺ cation represents a significant obstacle that has to be overcome; moreover, Na⁺ may be the reason why commercially available Al-rich ZSM-5 has a low concentration of Al pairs.^[11a,39c] Figure 18 reveals the effect of polarization and the addition of NaCl on the distribution of Al in ZSM-5 synthesized by using tetraethyl orthosilicate (TEOS) as the Si source and tetrapropylammonium hydroxide (TPAOH) as the SDA.

5.3. Composition of the aluminosilicate pool in the synthesis mixture

Recent results have indicated that in the synthesis of zeolites from mixtures/gels, the mixtures do not decompose into individual AlO₄⁻ or SiO₄ tetrahedra, but a significant fraction of larger aluminosilicate species (e.g., linear AlSi chains with at least 5 T atoms in the case of SSZ-13) is used to construct the new zeolite framework and is transferred from the synthesis mixture to the framework of the zeolite products. Thus, speciation of aluminosilicate species and the arrangement of Al atoms in the synthesis mixture can affect the organization of Al in the zeolite framework. Several methods can be employed to tune the organization of Al in the synthesis gel.

The presence (or current formation) of isolated AlO₄⁻ in the synthesis mixture significantly supports the formation of isolated Al atoms in the framework. The presence of isolated, not networked Al atoms can result from the use of Na silicate as the Si source, as in this case for which the Si source is already networked. Conversely, the incorporation of Al atoms into the silicate framework is difficult.

Even so, a high concentration of close Al atoms in the synthesis mixture, also including a fraction of AlSi₂Al sequences, can result in a significant increase in Al pairs in the zeolite framework. The increase in AlSi₂Al sequences can simply be reached by changing the mixing order during the preparation of the synthesis mixture. The addition of TPAOH to a well-mixed mixture of an Al salt and TEOS results in a lower fraction of Al pairs in the ZSM-5 product compared to the synthesis in which TEOS and TPAOH are added first. In the former case, a homogeneous distribution of Al atoms in the mixture minimizes the formation of AlSi₂Al sequences in the Si-rich gel, where-

as partial networking of TEOS in a basic environment after the addition of TPAOH results in a non-homogeneous gel with a fraction that is significantly enriched by Al.^[11a,39c]

A more sophisticated but extremely powerful variation of the above method that is based on a high concentration of AlSi₂Al sequences in the synthesis gel is the so-called “Al-rich gel” method, which is able to provide ZSM-5 samples with more than 90% of Al in pairs for Si/Al up to 60. In this case, the enrichment of the synthesis gel by AlSi₂Al sequences is reached by preparing the gel by mixing the two components, that is, an all-silica gel and a gel so rich in Al that AlSi₂Al sequences must be significantly present in it (e.g., for ZSM-5, the optimum Si/Al ratio for an Al-rich gel is close to 7).^[11a,43]

Another possible way to maximize or minimize the concentration of AlSi₂Al sequences in the synthesis gel is to select a zeolite with a proper Al distribution if the parent zeolite serves as the source of Al and Si for the synthesis (e.g., synthesis of SSZ-13). In this case, larger zeolite fragments are transferred from the parent zeolite through the stage of the synthesis mixture to the zeolite product.^[17c]

Notably, none of these methods represents a universal approach that can be applied for all types of zeolites, although the “Al-rich gel” method appears to be the most universal one. Nevertheless, in some cases the combination of the above methods results in the successful synthesis of zeolites with a (semi)monomodal Al distribution.

6. Al Distribution and Catalysis

The development of methods to tune the Al distribution in the zeolite and mainly to analyze the Al distribution represents a necessary starting point for elucidation of the relationship between the Al distribution and the activity as well as the selectivity of the zeolite catalyst. Although a significant step forward has recently been taken in this field, our knowledge regarding the effect of the Al distribution on catalyst performance is rather limited, especially in the field of acid-catalyzed reactions. This is due to the fact that redox metal ion/metal-oxo centers represent the only active sites in redox reactions over metallo-zeolites.^[8a,38,41c,52] Moreover, in the case of N₂O and NO_x abatement, the reactants are small molecules. Thus, the effect of the

Al distribution on the properties and the concentration of the redox cationic centers cannot be significantly affected or overlapped by other parameters of the metallozeolite catalyst. Conversely, the activity and mainly the selectivity of acid-catalyzed hydrocarbon transformations can be significantly affected by a number of other parameters, including the crystal size and the morphology, the presence of competing acid sites (Lewis Al sites), defects formed on the internal or external surfaces, differences in the concentrations and properties of the active sites on the outer and inner surfaces, and the location of the active sites in the zeolite channel system. Thus, conducting a study of the impact of the Al distribution on acid-catalyzed reactions is extremely difficult. Therefore, with the exception of a few studies, we can only speculate on the effect of the Al distribution in the field of acid catalysis.

It has to be pointed out that there are several ways how the Al distribution in the framework of protonic forms of zeolites can affect the properties of zeolite catalysts and, thus, their activity and selectivity in acid-catalyzed reactions. Besides the distance of acid sites, the types of acid sites and their acid strength are also suggested to affect the performance of zeolite catalysts.

6.1. Al distribution and type of acid sites

Although Brønsted acid sites of the Al–OH–Si bridging group predominantly represent acid sites in zeolite catalysts, Al Lewis sites can also be present in the protonic forms of zeolites. It is generally accepted that the presence of Al Lewis sites in zeolite catalysts is key in terms of the selectivity of the catalyst and in specific cases for which Lewis acid sites are also required for catalyst activity (e.g., Meerwein–Ponndorf–Verley reduction).^[53] Two types of Al Lewis sites have been reported for zeolites, that is, extra-framework Al Lewis sites and framework Al Lewis sites.^[8a]

Extra-framework Al Lewis sites represent extra-framework Al species located in the zeolite channel system. They can be formed in the zeolite intentionally by the release of framework Al atoms from the framework by steaming the parent zeolite (e.g., USY) or unintentionally as a result of dealumination occurring during template removal (typically in the case of beta zeolites). It has been shown that single Al atoms are released preferentially from the framework during calcination, whereas Al pairs are preserved in the framework in the case of beta zeolites.^[15,21] This suggests that the Al distribution represents an important parameter affecting the stability of Al in the zeolite framework. Thus, the presence of extra-framework Al Lewis sites is assumed to be significantly less pronounced in samples with Al pairs than in samples with prevailing single Al atoms after calcination under the same conditions. Nevertheless, it has to be mentioned that the formation of extra-framework Al Lewis sites can be avoided by careful template removal, even in the case of beta zeolites as opposed to the steaming procedure.

Framework Al Lewis sites are formed in substantial amounts only in beta zeolites. This type of Al Lewis site corresponds to perturbed, approximately planar framework Al atoms three co-

ordinated to the zeolite framework in the dehydrated zeolite.^[54] Upon rehydration, the structure of the zeolite framework is at least partially recovered, and the Al atoms are not leached from the zeolite. The significant formation of framework Al Lewis sites in beta zeolites with $\text{Si}/\text{Al} < 18$ correlates with another unique property of beta zeolites related to Al—the presence of close unpaired Al atoms. DFT calculations have shown that two Al atoms separated by three or four Si atoms in AlSiAlSi sequences are essential for opening the framework, enabling access of a guest molecule/reactant to the framework Al atoms without releasing some T atoms from the framework.^[55] This allows us to suggest that the presence of close, unpaired Al atoms in the zeolite is a necessary condition for the formation of framework Al Lewis sites in dehydrated zeolites.

6.2. Al distribution and strength of Brønsted acid sites

Discussion of the acid strength of the Brønsted acid sites in zeolites and its variability is still ongoing. It is undisputed that the strength of Brønsted protons in Al-rich zeolites with prevailing AlSiAl sequences is significantly weaker than that in Si-rich matrices. Sierka et al. showed that the acidity of Brønsted acidic sites was primarily determined by Al-for-Si substitutions in the nearest neighborhood of the Si atom of the Al–O(H)–Si bridge. The role of other next-nearest neighbor Al atoms is less important.^[56] Notably, the effect of AlSiAl sequences on the acid strength of protonic sites is not a key issue affecting the Al distribution, as these Al species are only rarely observed in Si-rich zeolites.

The abovementioned calculations indicate that a significant effect of the vicinity of a second Al atom in the Al pair on the acid strength (deprotonization energy or desorption of ammonia) of related protons cannot be supposed. The change in the local geometry of the Al–OH–Si site between an isolated Al atom and Al atoms in pairs is supposed not to be significantly higher than the variability in the Al–OH–Si arrangement connected with the location of Al–OH–Si sites in matrices with different topologies. This suggestion is confirmed by the fact that according to our knowledge the differences in acid properties (¹H chemical shift, OH stretching vibration, and vibrations of adsorbed [D₃]acetonitrile or pyridine) are not observed for ZSM-5 zeolites with prevailing single Al atoms and Al pairs.^[57] Thus, whereas close unpaired Al atoms can be associated with the formation of framework Al Lewis sites, both single Al atoms and Al atoms in Al pairs provide, according to contemporary knowledge, Brønsted acid sites with indistinguishable acid strengths.

6.3. Al distribution and distances of acid sites

In fact, the distance of acid sites is unambiguously given by the Al–Al distance only in the case of two framework Al Lewis sites.

In the case of the distance of two Brønsted acid sites, it has to be taken in account that the protons of these sites can be coordinated to any oxygen atom of the AlO_4^- tetrahedron. Be-

cause significant energy barriers have been reported for some cases for the migration of protons between oxygen atoms of the same AlO_4^- tetrahedron,^[58] the protons should, in these cases, be strictly correlated to the individual oxygen atoms. Thus, the proton distance is rather unclear, as two Brønsted protons can be, on the one hand, at the same distance for both the AlSiAl and AlSi_3Al sequences and, on the other hand, the distances between protons in the Al pair can significantly differ (even twice). Thus, the exact proton–proton distance can be obtained only by using a proton correlation NMR spectroscopy experiment (see Section 3). Nevertheless, this type of experiment also cannot provide exact information on the distance of acid sites in the catalysts under the reaction conditions. The elevated temperatures of catalytic reactions are most likely high enough to allow the barrier (if present) for proton migration to be overcome. Moreover, for the majority of Al species with two Al atoms, their exact arrangement in the framework is not known (with the exception of ferrierite and SSZ-13). Thus, the distances of acid sites only roughly correlate with the distances of the Al atoms in the zeolite, and information on the Al distribution represents only an indicative parameter in discussing a cooperation of the acid sites of AlSiAl sequences, Al pairs, and close unpaired Al atoms. Similar conclusions can also be drawn for cases in which framework Al Lewis sites and Brønsted acid sites are present in the catalyst. Whereas the position of the Al Lewis site is given by the Al distribution, its distance to the Brønsted site only roughly reflects the Al distribution.

For a reaction catalyzed by extra-framework Al Lewis sites by the cooperation of framework Al Lewis sites or Brønsted acid sites with these extra-framework Al Lewis sites, the effect of the Al distribution has also been suggested. Nevertheless, the Al distribution after dealumination has to be taken into account. Although the detailed structure of extra-framework Al Lewis sites is not known, it is suggested that they represent positively charged extra-framework species. Thus, they will be located in a dehydrated zeolite in the vicinity of framework Al atoms to compensate their negative charge. Thus, the distance of the framework and extra-framework acid sites in the catalyst represents the distance between the cationic position and the protonic site, and it is also driven by the Al distribution.

6.4. The distances of acid sites and catalysis

Because of limited information concerning the effect of the Al distribution on the catalytic performance of zeolite catalysts, the three mechanisms discussed below are speculative and require further experimental confirmation.

It is supposed that a reaction mechanism over an isolated acid site should vary from the bicentric one. Such a mechanism of the effect of the Al distribution should be reflected not only in the reaction rate but also by a significant effect on reaction selectivity.

A second possible mechanism represents the possibility that the reaction occurs on one center and that a second acid site serves as a reservoir for the substrate. The effect of the Al dis-

tribution on the course of the reaction should, in this case, also be reflected in both the rate and the selectivity.

Surprisingly, the only two experimentally proven mechanisms for control of the reaction by the Al distribution involve the effect of the second acid site on catalyst activity.^[12,33b,59]

1) The proximity of two protons results in pronounced polarization of alkanes, and this gives rise to a more positive apparent activation entropy. Both the reaction rate and selectivity are affected by Al organization.^[33b] 2) The vicinity of the second center should facilitate substrate adsorption or product desorption, whereas the reaction should occur identically on both the isolated acid sites and the two close acid sites. In this case, only the rate of the reaction is affected, and the selectivity of the reaction remains unchanged by the Al distribution.

6.5. Case examples of the effect of the Al distribution on the performance of zeolite catalysts

The number of these studies is significantly limited because of two reasons. First, the preparation of catalysts with different Al distributions and all other properties unchanged is a difficult task. Second, it is extremely difficult to distinguish between the effect of the Al distribution and the effect of shape selectivity resulting from different Al sitings. Thus, only zeolites with a simple cavity system or catalysts with an analyzed Al siting can be employed for this purpose.

6.5.1. Oligomerization of propene over H-ZSM-5

The development of procedures to control the Al distribution by zeolite synthesis and the analysis of the Al siting in ZSM-5 samples synthesized by using TPA^+ cations as the SDA has enabled detailed study of the effects of single Al atoms and Al pairs on oligomerization reactions for $\text{Si}/\text{Al}=12\text{--}30$. Note that in the synthesis with TPA^+ cations, the Al atoms are located predominantly at the channel intersections, and the shape selectivity effect of Al located in the ZSM-5 channels is suppressed. The rate of propene oligomerization by zeolites with a monomodal distribution of Al pairs is up to eight times higher than that by samples exclusively containing single Al atoms.^[12] Relative to the activity of commercial samples, the activity of catalysts with Al pairs is four times higher. Conversely, the selectivity of the reaction is the same for both types of catalysts. An FTIR spectroscopy study including operando conditions has clearly shown that all steps of the intrinsic reaction, as well as the steps for the adsorption of the substrate molecule to the protonic site, proceed faster on isolated protonic sites. Nevertheless, decomposition of the late transition state and release of the products to the gas phase occur significantly faster from the close centers of the Al pairs, causing the observed higher activity for samples with Al pairs.

6.5.2. Cracking of hydrocarbons

In the cracking of 1-butene over H-ZSM-5, a set of samples with $\text{Si}/\text{Al}=12\text{--}40$ prepared by using TPA^+ and thus having Al atoms at the intersection have been studied. Marked differen-

ces in the yield and selectivity in the cracking of 1-butene are observed (note that the conditions for the reaction are different, and the conversion of the substrate is significantly higher than that for propene oligomerization). Distant single protons support cracking of butene and octene (formed by dimerization). Close protonic sites enhance oligomerization and hydrogen-transfer reactions leading to aromatics.^[57] Figure 19 reveals the effect of the Al distribution on the cracking of 1-butene.

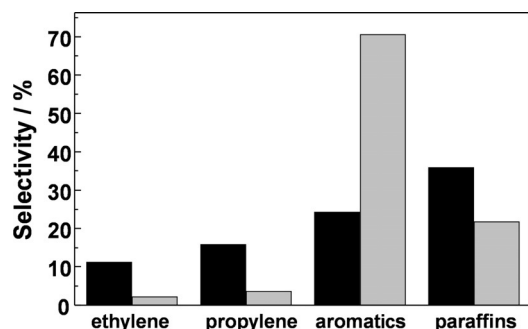


Figure 19. Effect of the Al distribution on the cracking of 1-butene over ZSM-5 with Si/Al = 15 and 84% (■) and 40% (▨) of single Al. $T = 500\text{ }^{\circ}\text{C}$, time on stream: 20 min; gas hourly space velocity: 15 h^{-1} .

Similarly, the effect of the Al distribution on product selectivity has been reported for the cracking of liquefied petroleum gas to ethylene and propylene. Greater yields of olefins are reported for samples with higher fractions of single Al atoms, whereas greater yields of C_{5+} alkanes and coke are associated with Al pairs.^[60]

In the cracking of alkanes (propane, *n*-butane, and *n*-pentane), close protonic sites in ZSM-5 catalyze the reaction at higher turnover rates than the isolated ones. ^{13}C MAS NMR spectroscopy evidences more pronounced polarization of the alkanes in zeolites with close Brønsted acid sites. This results in similar apparent activation energies for the catalysts with single Al and Al pairs. Conversely, more positive apparent activation entropies are connected with Al pairs. DFT calculations, confirmed by catalytic tests, prove that higher cracking rates at Al pairs are mainly due to more positive intrinsic activation entropies, which suggests that the protonation transition state occurs later along the reaction coordinate on adjacent Brønsted

acid sites. Moreover, the Al distribution also affects the selectivity of this reaction. Al pairs favor cracking over dehydrogenation and favor central cracking over terminal cracking.^[33b] Figure 20 shows the effect of Al pairs and single Al atoms on the formation of H-bonded C_3H_6 and on the reaction rate for C_3H_6 oligomerization to C_4 – C_9 olefins (C).

6.5.3. Methanol-to-olefin (MTO) reactions over SSZ-39 and SSZ-13

Dealumination of the SSZ-39 zeolite has been reported to significantly decrease the number of close Al atoms (Al pairs and close unpaired Al atoms are not discriminated in the study) in the framework. The decrease in the total Al content and in the concentration of Al pairs results in effective olefin-producing catalysts. Conversely, the presence of close Al atoms results in the formation of higher alkanes and carbonaceous deposits under the same reaction conditions. Although it is not possible to distinguish the effect of the decrease in the Al content from the decrease in Al pairs on catalyst performance, the simple cavity system with the AEI topology of SSZ-39 excludes the effect of the position in the channel system.^[7]

The significant effect of the Al distribution in the catalyst on MTO reactions has been further confirmed for SSZ-13. In this zeolite with CHA topology, only one T atom forms the framework with only one type of large cavity. Fewer close Al atoms (Al pairs or close unpaired Al) in dealuminated samples lead to more stable light olefin selectivity, with a reduced initial transient period, lower initial propane selectivity, and longer catalyst lifetime. The crucial role of the Al distribution in MTO reactions and the exclusion of the substantial role of the total Al content have been confirmed by the selective dealumination of samples to provide species with a lower framework Al content but with preserved Al pairs.^[36b]

7. Outlook

As shown in the previous sections, the main limits to employing the distribution of Al to control acid-catalyzed reactions over zeolites have been overcome. Methods to tune the Al distribution in the zeolite framework and methods to analyze the Al distribution in prepared catalysts have been successfully developed. Nevertheless, many challenges in this field remain.

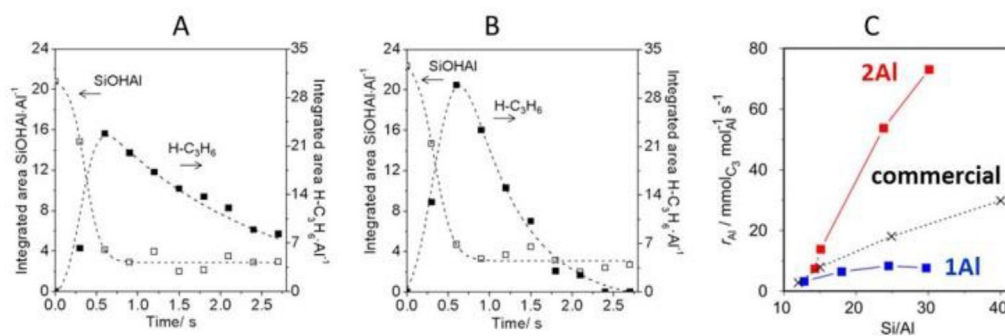


Figure 20. The effect of a) Al pairs and b) single Al atoms on the formation of H-bonded C_3H_6 and c) on the reaction rate for C_3H_6 oligomerization to C_4 – C_9 olefins.

The effect of the Al distribution has, to date, only been studied for a few types of reactions—cracking and oligomerization of alkenes and MTO reactions—and only for ZSM-5, SSZ-13, and SSZ-39. Thus, there is plenty of room from the points of view of reactions and topologies of zeolite matrices, including industrially widely applied matrices such as beta zeolites, mordenites, ferrierites, and MCM-22.

We can say that the management of the Al distribution has been fully mastered only for the ZSM-5 zeolite. Some partial success has been achieved for beta zeolites and small-pore zeolites such as SSZ-13 and SSZ-39. For ferrierites and MCM-22 zeolites, it has only been demonstrated that the Al distribution in these matrices can be tuned. Thus, there is a broad untouched area for the development of new catalysts with a tuned Al distribution. Note that there is a set of methods that enable tuning the Al distribution. Nevertheless, their applicability for the synthesis of individual matrices has to be elucidated, as does the effect of the combination of several approaches.

As shown for the cracking of 1-butene and MTO reactions, the Al distribution can significantly affect the selectivity of the reaction towards large molecules and coke deposits. This opens the possibility to design highly stable catalysts by tuning the Al distribution. The effect of the Al distribution on the formation of Al Lewis sites, which often favor the formation of carbon deposits, also cannot be omitted in this field.

Preliminary results indicate that the Al distribution in a zeolite can significantly affect the stability of the Al atoms in the framework. Perturbation of the framework during zeolite treatment can result in the formation of framework Al Lewis sites and in the leaching of Al atoms from the framework, which results in the creation of extra-framework Al Lewis sites. On the one hand, this suggests the possibility to control the nature of the acid sites by tuning the Al distribution. On the other hand, this effect can be employed to tune the Al distribution in the framework if attempts to tune the Al distribution by synthesis do not provide appropriate results. Notably, successful accomplishment of the above tasks will also benefit the area of redox catalysis over metallozeolites.

8. Summary

Various arrangements of framework Al atoms in Si-rich zeolites are possible. The following Al species are significant because of the effect of the arrangement of Al atoms on the properties of acid catalysts: First, Al atoms in such an arrangement that their related acid sites can be regarded as isolated without the possibility to cooperate in the reaction. Single Al atoms (not able to accommodate divalent cationic complexes in hydrated zeolites) and AlSiAl sequences separated by zeolite walls belong to this class. Second, Al atoms close enough that their acid sites can cooperate. Al pairs of AlSi_{2,3}Al sequences located in one ring and accommodating bare divalent cations in dehydrated zeolites and close unpaired Al atoms that are able to accommodate only divalent cationic complexes in hydrated zeolites belong to this group, as well as AlSiAl sequences facing the same channel or cavity.

Several experimental approaches have been developed to analyze the Al distribution in zeolite frameworks. The most effective way to analyze the Al distribution involves the combination of ²⁹Si MAS NMR spectroscopy with FTIR and Vis spectroscopy of Co²⁺ cations as probes in hydrated and dehydrated zeolites. ²⁹Si MAS NMR spectroscopy can be employed to evidence AlSiAl sequences, whereas Co²⁺ cations enable the monitoring of single Al atoms, close unpaired Al atoms, and Al pairs. Theoretical methods based on the application of a statistical approach or on the prediction of the stabilization energy of Al atoms in individual arrangements cannot be employed to predict the Al organization in zeolite frameworks.

AlSiAl sequences have been reported only for a few types of Si-rich zeolites (ZSM-5, beta, SSZ-13) with higher framework Al contents (Si/Al < 10). Close unpaired Al atoms are known only for SSZ-13 and beta zeolites with Si/Al < 18. Conversely, both single Al atoms and Al pairs can be found in various topologies, independent of the framework Al content.

The distribution of Al atoms between the individual Al species is, in general, not random or controlled by simple rules or the framework Al content but depends on the conditions used for zeolite synthesis. Al pairs can prevail in zeolites with low framework Al contents, whereas single Al atoms can predominate in Al-rich samples of the same topology. Thus, matrices of the same topology and framework Al content can dramatically differ in the concentrations of the individual Al species, as it was reported for ZSM-5, mordenite, ferrierite, beta zeolite, MCM-22, and SSZ-13. The distribution of Al atoms in the zeolite product is affected by several parameters during the synthesis. Polarization of the template, the presence of inorganic co-cations, Al organization in the synthesis mixture obtained by controlling the Si source, and the order of mixing the individual components of the gel have all been reported to affect the Al distribution. This enables the synthesis of zeolites with a (semi)monomodal Al distribution (with one type of Al species significantly prevailing), as it was demonstrated for ZSM-5, SSZ-13, and beta zeolites. Methods for tuning the Al distribution are well developed for the ZSM-5 zeolite, which can be prepared with any distribution of single Al and Al pairs over a broad range of framework Al contents (Si/Al = 13–60). Methods for substantial tuning the Al distribution have also been reported for beta zeolite and SSZ-13.

The crucial effect of the Al distribution on catalytic performance has mainly been reported for zeolites containing transition-metal cations applied as catalysts in redox reactions. Nevertheless, it has unambiguously been shown that the Al distribution can also markedly affect the activity and selectivity of zeolite catalysts in acid-catalyzed reactions. Besides the direct effect of the (non)cooperation of two acidic centers in the reaction, the Al distribution can also affect the nature of the active sites. The effect of the Al distribution on the formation of framework and extra-framework Al Lewis sites has been reported for some zeolites.

Methods for both the analysis of the Al distribution in the zeolite framework and for its control by governing the conditions of the synthesis have successfully been developed for some industrially relevant zeolite matrices. Thus, tuning the Al

distribution in the zeolite framework can be employed to optimize the properties of the zeolite catalysts towards the requirements of individual reactions. The significant effect of the Al distribution on catalyst activity and selectivity has clearly been demonstrated for the oligomerization of propylene, the cracking of butane, and methanol-to-olefins reactions. Because individual Al species are in some amount present in the zeolite, tuning the Al distribution cannot represent a really dramatic breakthrough in zeolite activity. Nevertheless, an increase in the activity/selectivity ranging from many tens of percent up to one magnitude should make it easier to reach the catalyst/process parameters that are required for industrial applications. A significant advantage connected with optimization of zeolite properties for the development of new highly active, selective, and stable catalysts and catalytic processes by tuning the Al distribution is that neither the synthesis of zeolites with a tuned Al distribution nor the technology of the catalytic process itself require substantial changes compared to the standard catalyst synthesis and technology.

Acknowledgements

This work was supported by the Grant Agency of the Czech Republic under projects: # 17-00742S and the RVO: 61388955.

Conflict of interest

The authors declare no conflict of interest.

Keywords: aluminum · catalytic activity · FTIR spectroscopy · NMR spectroscopy · zeolites

- [1] J. Weitkamp, M. Hunger in *Introduction to Zeolite Science and Practice (Studies in Surface Science and Catalysis)* (Eds.: J. Cejka, H. van Bekkum, A. Corma, F. Schüth), Elsevier, Amsterdam, **2007**, Vol. 168, pp. 787–835.
- [2] a) A. Corma, *Chem. Rev.* **1995**, *95*, 559–614; b) A. Primo, H. Garcia, *Chem. Soc. Rev.* **2014**, *43*, 7548–7561; c) E. T. C. Vogt, B. M. Weckhuysen, *Chem. Soc. Rev.* **2015**, *44*, 7342–7370.
- [3] a) A. M. Beale, F. Gao, I. Lezcano-Gonzalez, C. H. F. Peden, J. Szanyi, *Chem. Soc. Rev.* **2015**, *44*, 7371–7405; b) S. Roy, M. S. Hegde, G. Madras, *Appl. Energy* **2009**, *86*, 2283–2297; c) W. P. Shan, H. Song, *Catal. Sci. Technol.* **2015**, *5*, 4280–4288.
- [4] a) P. Bhanja, A. Bhaumik, *Fuel* **2016**, *185*, 432–441; b) T. Ennaert, J. Van Aelst, J. Dijkman, R. De Clercq, W. Schutyser, M. Dusselier, D. Verboeckend, B. F. Sels, *Chem. Soc. Rev.* **2016**, *45*, 584–611; c) T. J. Schwartz, B. J. O'Neill, B. H. Shanks, J. A. Dumesic, *ACS Catal.* **2014**, *4*, 2060–2069.
- [5] a) Z. F. Bian, S. Das, M. H. Wai, P. Hongmanorom, S. Kawi, *ChemPhysChem* **2017**, *18*, 3117–3134; b) E. Catizzone, G. Bonura, M. Migliori, F. Frusteri, G. Giordano, *Molecules* **2018**, *23*, 31; c) K. Narsimhan, K. Iyoki, K. Dinh, Y. Roman-Leshkov, *ACS Cent. Sci.* **2016**, *2*, 424–429; d) M. Ravi, M. Ranochiari, J. A. van Bokhoven, *Angew. Chem. Int. Ed.* **2017**, *56*, 16464–16483; *Angew. Chem.* **2017**, *129*, 16684–16704; e) B. E. R. Snyder, M. L. Bols, R. A. Schoonheydt, B. F. Sels, E. I. Solomon, *Chem. Rev.* **2018**, *118*, 2718–2768; f) Z. Zakaria, S. K. Kamarudin, *Renewable Sustainable Energy Rev.* **2016**, *65*, 250–261.
- [6] a) R. M. Barrer, *Hydrothermal Chemistry of Zeolites*, Academic Press, London, **1982**; b) *Introduction to Zeolite Science and Practice (Studies in Surface Science and Catalysis)* (Eds.: H. van Bekkum, E. M. Flanigen, J. C. Jansen), Elsevier, Amsterdam, Vol. 58, **1991**.
- [7] *Database of Zeolite Structures*, <http://www.iza-structure.org/databases> (accessed December 17, 2018)..
- [8] a) J. Dědeček, Z. Sobalik, B. Wichterlova, *Catal. Rev. Sci. Eng.* **2012**, *54*, 135–223; b) E. G. Derouane, J. C. Vadrine, R. R. Pinto, P. M. Borges, L. Costa, M. Lemos, F. Lemos, F. R. Ribeiro, *Catal. Rev. Sci. Eng.* **2013**, *55*, 454–515; c) D. P. Serrano, J. A. Melero, G. Morales, J. Iglesias, P. Pizarro, *Catal. Rev. Sci. Eng.* **2018**, *60*, 1–70.
- [9] a) M. Boronat, C. Martinez-Sanchez, D. Law, A. Corma, *J. Am. Chem. Soc.* **2008**, *130*, 16316–16323; b) S. Sklenak, J. Dědeček, C. B. Li, B. Wichterlova, V. Gabova, M. Sierka, J. Sauer, *Angew. Chem. Int. Ed.* **2007**, *46*, 7286–7289; *Angew. Chem.* **2007**, *119*, 7424–7427.
- [10] a) J. Dědeček, D. Kaucky, B. Wichterlova, *Chem. Commun.* **2001**, 970–971; b) B. C. Knott, C. T. Nimlos, D. J. Robichaud, M. R. Nimlos, S. Kim, R. Gounder, *ACS Catal.* **2018**, *8*, 770–784.
- [11] a) J. Dědeček, V. Balgova, V. Pashkova, P. Klein, B. Wichterlova, *Chem. Mater.* **2012**, *24*, 3231–3239; b) V. Gábová, J. Dědeček, J. Cejka, *Chem. Commun.* **2003**, 1196–1197.
- [12] M. Bernauer, E. Tabor, V. Pashkova, D. Kaucky, Z. Sobalik, B. Wichterlova, J. Dědeček, *J. Catal.* **2016**, *344*, 157–172.
- [13] W. Loewenstein, *Am. Mineral.* **1954**, *39*, 92–96.
- [14] a) E. Lippmaa, M. Magi, A. Samoson, M. Tarmak, G. Engelhardt, *J. Am. Chem. Soc.* **1981**, *103*, 4992–4996; b) M. T. Melchior, D. E. W. Vaughan, A. J. Jacobson, *J. Am. Chem. Soc.* **1982**, *104*, 4859–4864.
- [15] J. Dědeček, L. Čapek, D. Kaucky, Z. Sobalik, B. Wichterlova, *J. Catal.* **2002**, *211*, 198–207.
- [16] K. Mlekodaj, J. Dědeček, V. Pashkova, E. Tabor, P. Klein, M. Urbanova, R. Karcz, P. Szazama, S. R. Whittleton, H. M. Thomas, A. V. Fishchuk, S. Sklenak, *J. Phys. Chem. C* **2018**, <https://doi.org/10.1021/acs.jpcc.8b07343>.
- [17] a) J. Dědeček, S. Sklenak, C. Li, B. Wichterlova, V. Gabova, J. Brus, M. Sierka, J. Sauer, *J. Phys. Chem. C* **2009**, *113*, 1447–1458; b) C. A. Fyfe, G. C. Gobbi, G. J. Kennedy, *J. Phys. Chem.* **1984**, *88*, 3248–3253; c) K. Mlekodaj, V. Pashkova, M. Urbanova, E. Tabor, P. Klein, J. Dědeček, unpublished results; d) P. Szazama, E. Tabor, P. Klein, B. Wichterlova, S. Sklenak, L. Mokrzycki, V. Pashkova, M. Ogura, J. Dědeček, *J. Catal.* **2016**, *333*, 102–114.
- [18] J. Dědeček, D. Kaucky, B. Wichterlova, O. Gonsiorova, *Phys. Chem. Chem. Phys.* **2002**, *4*, 5406–5413.
- [19] L. Čapek, J. Dědeček, P. Szazama, B. Wichterlova, *J. Catal.* **2010**, *272*, 44–54.
- [20] L. Benco, T. Bucko, J. Hafner, H. Toulhoat, *J. Phys. Chem. B* **2005**, *109*, 20361–20369.
- [21] L. Čapek, J. Dědeček, B. Wichterlova, *J. Catal.* **2004**, *227*, 352–366.
- [22] a) W. J. Mortier, J. J. Pluth, J. V. Smith, *Mater. Res. Bull.* **1977**, *12*, 97–102; b) D. H. Olson, *J. Phys. Chem.* **1968**, *72*, 4366–4373; c) J. V. Smith, *Acta Crystallogr.* **1962**, *15*, 835–845; d) A. A. Verberckmoes, B. M. Weckhuysen, J. Pelgrims, R. A. Schoonheydt, *J. Phys. Chem.* **1995**, *99*, 15222–15228.
- [23] S. Sklenak, P. C. Andrikopoulos, B. Boekfa, B. Jansang, J. Novakova, L. Benco, T. Bucko, J. Hafner, J. Dědeček, Z. Sobalik, *J. Catal.* **2010**, *272*, 262–274.
- [24] R. Karcz, J. Dědeček, B. Supronowicz, H. M. Thomas, P. Klein, E. Tabor, P. Szazama, V. Pashkova, S. Sklenak, *Chem. Eur. J.* **2017**, *23*, 8857–8870.
- [25] a) G. Engelhardt, U. Lohse, E. Lippmaa, M. Tarmak, M. Magi, *Z. Anorg. Allg. Chem.* **1981**, *482*, 49–64; b) J. Klinowski, S. Ramdas, J. M. Thomas, C. A. Fyfe, J. S. Hartman, *J. Chem. Soc. Faraday Trans. 2* **1982**, *78*, 1025–1050.
- [26] a) M. J. Duer, *Solid State NMR Spectroscopy: Principles and Applications*, Blackwell Science, Oxford, **2002**; b) G. Engelhardt, D. Michel, *High-Resolution Solid State NMR of Silicates and Zeolites*, Wiley, New York, **1987**; c) K. J. D. Mackenzie, M. E. Smith, *Multinuclear Solid State NMR of Inorganic Materials*, Elsevier, Oxford, **2002**.
- [27] C. Martineau-Corcoss, J. Dědeček, F. Taulelle, *Solid State Nucl. Magn. Reson.* **2017**, *84*, 65–72.
- [28] G. Mali, F. Taulelle, *Chem. Commun.* **2004**, 868–869.
- [29] Z. W. Yu, A. M. Zheng, Q. A. Wang, L. Chen, J. Xu, J. P. Amoureux, F. Deng, *Angew. Chem. Int. Ed.* **2010**, *49*, 8657–8661; *Angew. Chem.* **2010**, *122*, 8839–8843.
- [30] a) Z. W. Yu, S. H. Li, Q. Wang, A. M. Zheng, X. Jun, L. Chen, F. Deng, *J. Phys. Chem. C* **2011**, *115*, 22320–22327; b) Z. W. Yu, Q. Wang, L. Chen, F. Deng, *Chin. J. Catal.* **2012**, *33*, 129–139.
- [31] a) J. Dědeček, M. J. Lucero, C. B. Li, F. Gao, P. Klein, M. Urbanova, Z. Tvaruzkova, P. Szazama, S. Sklenak, *J. Phys. Chem. C* **2011**, *115*, 11056–11064; b) S. Sklenak, J. Dědeček, C. Li, F. Gao, B. Jansang, B. Boekfa, B. Wichter-

- lova, J. Sauer, *Collect. Czech. Chem. Commun.* **2008**, *73*, 909–920; c) S. Sklenak, J. Dědeček, C. Li, B. Wichterlova, V. Gabova, M. Sierka, J. Sauer, *Phys. Chem. Chem. Phys.* **2009**, *11*, 1237–1247; d) A. Vjunov, J. L. Fulton, T. Huthwelker, S. Pin, D. Mei, G. K. Schenter, N. Govind, D. M. Camaioni, J. Z. Hu, J. A. Lercher, *J. Am. Chem. Soc.* **2014**, *136*, 8296–8306; Corrigendum: A. Vjunov, J. L. Fulton, T. Huthwelker, S. Pin, D. H. Mei, G. K. Schenter, N. Govind, D. M. Camaioni, J. Z. Hu, J. A. Lercher, *J. Am. Chem. Soc.* **2015**, *137*, 2409.
- [32] H. Koller, S. Senapati, J. J. Ren, T. Uesbeck, V. Siozios, M. Hunger, R. F. Lobo, *J. Phys. Chem. C* **2016**, *120*, 9811–9820.
- [33] a) S. H. Li, A. M. Zheng, Y. C. Su, H. L. Zhang, L. Chen, J. Yang, C. H. Ye, F. Deng, *J. Am. Chem. Soc.* **2007**, *129*, 11161–11171; b) C. H. Song, Y. Y. Chu, M. Wang, H. Shi, L. Zhao, X. F. Guo, W. M. Yang, J. Y. Shen, N. H. Xue, L. M. Peng, W. P. Ding, *J. Catal.* **2017**, *349*, 163–174; c) A. Zheng, S. Li, S.-B. Liu, F. Deng, *Acc. Chem. Res.* **2016**, *49*, 655–663.
- [34] a) H. Koller, T. Uesbeck, M. R. Hansen, M. Hunger, *J. Phys. Chem. C* **2017**, *121*, 25930–25940; b) Z. C. Wang, L. Z. Wang, Y. J. Jiang, M. Hunger, J. Huang, *ACS Catal.* **2014**, *4*, 1144–1147.
- [35] A. B. P. Lever, *Inorganic Electronic Spectroscopy*, 2nd ed., Elsevier, Amsterdam, **1984**.
- [36] a) J. D. Albarracín-Caballero, I. Khurana, J. R. Di Iorio, A. J. Shih, J. E. Schmidt, M. Dusselier, M. E. Davis, A. Yezerets, J. T. Miller, F. H. Ribeiro, R. Gounder, *React. Chem. Eng.* **2017**, *2*, 168–179; b) M. A. Deimund, L. Harrison, J. D. Lunn, Y. Liu, A. Malek, R. Shayib, M. E. Davis, *ACS Catal.* **2016**, *6*, 542–550.
- [37] J. Dědeček, B. Wichterlova, *J. Phys. Chem. B* **1997**, *101*, 10233–10240.
- [38] J. Dědeček, L. Čapek, P. Sazama, Z. Sobalik, B. Wichterlova, *Appl. Catal. A* **2011**, *391*, 244–253.
- [39] a) L. Čapek, V. Kreibich, J. Dědeček, T. Grygar, B. Wichterlova, Z. Sobalik, J. A. Martens, R. Brosius, V. Tokarova, *Microporous Mesoporous Mater.* **2005**, *80*, 279–289; b) L. Čapek, K. Novoveska, Z. Sobalik, B. Wichterlova, L. Cider, E. Jobson, *Appl. Catal. B* **2005**, *60*, 201–210; c) J. Dědeček, D. Kaucky, B. Wichterlova, *Microporous Mesoporous Mater.* **2000**, *35*–36, 483–494; d) L. Drozdová, R. Prins, J. Dědeček, Z. Sobalik, B. Wichterlova, *J. Phys. Chem. B* **2002**, *106*, 2240–2248; e) S. Sklenak, P. C. Andrikopoulos, S. R. Whittleton, H. Jirglova, P. Sazama, L. Bencko, T. Bucko, J. Hafner, Z. Sobalik, *J. Phys. Chem. C* **2013**, *117*, 3958–3968; f) E. Tabor, K. Jisa, J. Novakova, Z. Bastl, A. Vondrova, K. Zaveta, Z. Sobalik, *Microporous Mesoporous Mater.* **2013**, *165*, 40–47; g) E. Tabor, K. Závěta, N. K. Sathu, Z. Tvaržková, Z. Sobalik, *Catal. Today* **2011**, *169*, 16–23; h) E. Tabor, K. Zaveta, N. K. Sathu, A. Vondrova, P. Sazama, Z. Sobalik, *Catal. Today* **2011**, *175*, 238–244.
- [40] Z. Sobalik, J. Dědeček, D. Kaucky, B. Wichterlova, L. Drozdova, R. Prins, *J. Catal.* **2000**, *194*, 330–342.
- [41] a) M. Ogura, K. Itabashi, J. Dědeček, T. Onkawa, Y. Shimada, K. Kawakami, K. Onodera, S. Nakamura, T. Okubo, *J. Catal.* **2014**, *315*, 1–5; b) Z. Sobalik, A. A. Belhekar, Z. Tvaruzkova, B. Wichterlova, *Appl. Catal. A* **1999**, *188*, 175–186; c) Z. Sobalik, J. Dědeček, I. Ikonnikov, B. Wichterlova, *Microporous Mesoporous Mater.* **1998**, *21*, 525–532.
- [42] a) J. Dědeček, B. Wichterlova, *J. Phys. Chem. B* **1999**, *103*, 1462–1476; b) D. Kaucky, J. I. Dědeček, B. Wichterlova, *Microporous Mesoporous Mater.* **1999**, *31*, 75–87.
- [43] V. Pashkova, P. Klein, J. Dědeček, V. Tokarova, B. Wichterlova, *Microporous Mesoporous Mater.* **2015**, *202*, 138–146.
- [44] E. Dempsey, *J. Phys. Chem.* **1969**, *73*, 3660–3668.
- [45] a) T. Takaishi, M. Kato, K. Itabashi, *J. Phys. Chem.* **1994**, *98*, 5742–5743; b) T. Takaishi, M. Kato, K. Itabashi, *Zeolites* **1995**, *15*, 21–32.
- [46] V. Pashkova, S. Sklenak, P. Klein, M. Urbanova, J. Dědeček, *Chem. Eur. J.* **2016**, *22*, 3937–3941.
- [47] a) O. Bortnovsky, Z. Sobalik, B. Wichterlova, *Microporous Mesoporous Mater.* **2001**, *46*, 265–275; b) O. Bortnovsky, Z. Sobalik, B. Wichterlova, Z. Bastl, *J. Catal.* **2002**, *210*, 171–182.
- [48] Z. C. Zhao, Y. D. Xing, S. H. Li, X. J. Meng, F. S. Xiao, R. McGuire, A. N. Parvulescu, U. Muller, W. P. Zhang, *J. Phys. Chem. C* **2018**, *122*, 9973–9979.
- [49] a) J. R. Di Iorio, R. Gounder, *Chem. Mater.* **2016**, *28*, 2236–2247; b) J. R. Di Iorio, C. T. Nimlos, R. Gounder, *ACS Catal.* **2017**, *7*, 6663–6674.
- [50] S. Prasad, M. Petrov, *Solid State Nucl. Magn. Reson.* **2013**, *54*, 26–31.
- [51] T. Biligetü, Y. Wang, T. Nishitoba, R. Otomo, S. Park, H. Mochizuki, J. N. Rondo, T. Tatsumi, T. Yokoi, *J. Catal.* **2017**, *353*, 1–10.
- [52] B. Wichterlová, J. Dědeček, Z. Sobalik in *Catalysis by Unique Metal Ion Structures in Solid Matrices: From Science to Application* (Eds.: G. Centi, B. Wichterlová, A. T. Bell), Kluwer, Dordrecht, **2001**, pp. 31–53.
- [53] C. F. de Graauw, J. A. Peters, H. Vanbekkum, J. Huskens, *Synthesis* **1994**, 1007–1017.
- [54] J. Brus, L. Kobera, W. Schoefberger, M. Urbanova, P. Klein, P. Sazama, E. Tabor, S. Sklenak, A. V. Fishchuk, J. Dědeček, *Angew. Chem. Int. Ed.* **2015**, *54*, 541–545; *Angew. Chem.* **2015**, *127*, 551–555.
- [55] L. Kobera, J. Dedeczek, V. Pashkova, P. Klein, E. Tabor, M. Urbanova, J. Brus, H. M. Thomas, A. V. Fishchuk, S. Sklenak, unpublished results.
- [56] M. Sierka, U. Eichler, J. Datka, J. Sauer, *J. Phys. Chem. B* **1998**, *102*, 6397–6404; Corrigendum: M. Sierka, U. Eichler, J. Datka, J. Sauer, *J. Phys. Chem. B* **1998**, *102*, 10468.
- [57] P. Sazama, J. Dědeček, V. Gabova, B. Wichterlova, G. Spoto, S. Bordiga, *J. Catal.* **2008**, *254*, 180–189.
- [58] M. Sierka, J. Sauer, *J. Phys. Chem. B* **2001**, *105*, 1603–1613.
- [59] J. M. Findley, P. I. Ravikovitch, D. S. Sholl, *J. Phys. Chem. C* **2018**, *122*, 12332–12340.
- [60] S. Abbasizadeh, R. Karimzadeh, *Microporous Mesoporous Mater.* **2018**, *266*, 132–140.

Manuscript received: September 26, 2018
Version of record online: December 21, 2018